

**A measurement of the semileptonic
branching ratio $\text{BR}(\text{b-baryon} \rightarrow \text{pl}\bar{\nu}X)$
and a study of inclusive $\pi^\pm, \text{K}^\pm, (\text{p}, \bar{\text{p}})$
production in Z decays**

The ALEPH collaboration¹

Abstract

Inclusive π^\pm, K^\pm and $(\text{p}, \bar{\text{p}})$ production is investigated using data recorded by the ALEPH detector between 1992 and 1994. The momentum spectra and multiplicities are measured separately in $Z \rightarrow \text{b}\bar{\text{b}}, Z \rightarrow \text{c}\bar{\text{c}}$ and $Z \rightarrow \text{u}\bar{\text{u}}, \text{d}\bar{\text{d}}, \text{s}\bar{\text{s}}$ decays. The number of protons found in b-hadron decays is used to estimate the fraction of b-baryons in b events to be $(10.2 \pm 0.7 \pm 2.7)\%$. From an additional study of proton-lepton correlations in b events the branching ratio $\text{BR}(\text{b-baryon} \rightarrow \text{pl}\bar{\nu}X) = (4.63 \pm 0.72 \pm 0.98)\%$ is obtained. The ratio $\text{BR}(\text{b-baryon} \rightarrow \text{pl}\bar{\nu}X) / \text{BR}(\text{b-baryon} \rightarrow \text{p}X)$ is found to be $0.080 \pm 0.012 \pm 0.014$.

(Submitted to European Physical Journal C)

¹See the following pages for the list of authors

The ALEPH Collaboration

R. Barate, D. Buskalic, D. Decamp, P. Ghez, C. Goy, J.-P. Lees, A. Lucotte, M.-N. Minard, J.-Y. Nief, B. Pietrzyk

Laboratoire de Physique des Particules (LAPP), IN²P³-CNRS, 74019 Annecy-le-Vieux Cedex, France

G. Boix, M.P. Casado, M. Chmeissani, J.M. Crespo, M. Delfino, E. Fernandez, M. Fernandez-Bosman, Ll. Garrido,¹⁵ E. Graugès, A. Juste, M. Martinez, G. Merino, R. Miquel, Ll.M. Mir, I.C. Park, A. Pascual, J.A. Perlas, I. Riu, F. Sanchez

Institut de Física d'Altes Energies, Universitat Autònoma de Barcelona, 08193 Bellaterra (Barcelona), Spain⁷

A. Colaleo, D. Creanza, M. de Palma, G. Gelao, G. Iaselli, G. Maggi, M. Maggi, N. Marinelli, S. Nuzzo, A. Ranieri, G. Raso, F. Ruggieri, G. Selvaggi, L. Silvestris, P. Tempesta, A. Tricoli,³ G. Zito

Dipartimento di Fisica, INFN Sezione di Bari, 70126 Bari, Italy

X. Huang, J. Lin, Q. Ouyang, T. Wang, Y. Xie, R. Xu, S. Xue, J. Zhang, L. Zhang, W. Zhao

Institute of High-Energy Physics, Academia Sinica, Beijing, The People's Republic of China⁸

D. Abbaneo, R. Alemany, U. Becker, P. Bright-Thomas, D. Casper, M. Cattaneo, F. Cerutti, V. Ciulli, G. Dissertori, H. Drevermann, R.W. Forty, M. Frank, R. Hagelberg, J.B. Hansen, J. Harvey, P. Janot, B. Jost, I. Lehraus, P. Mato, A. Minten, L. Moneta, A. Pacheco, J.-F. Puztazzer,²³ F. Ranjard, L. Rolandi, D. Rousseau, D. Schlatter, M. Schmitt, O. Schneider, W. Tejessy, F. Teubert, I.R. Tomalin, H. Wachsmuth, A. Wagner²⁰

European Laboratory for Particle Physics (CERN), 1211 Geneva 23, Switzerland

Z. Ajaltouni, F. Badaud, G. Chazelle, O. Deschamps, A. Falvard, C. Ferdi, P. Gay, C. Guicheney, P. Henrard, J. Jousset, B. Michel, S. Monteil, J-C. Montret, D. Pallin, P. Perret, F. Podlyski, J. Proriot, P. Rosnet

Laboratoire de Physique Corpusculaire, Université Blaise Pascal, IN²P³-CNRS, Clermont-Ferrand, 63177 Aubière, France

T. Fearnley, J.D. Hansen, J.R. Hansen, P.H. Hansen, B.S. Nilsson, B. Rensch, A. Wäänänen

Niels Bohr Institute, 2100 Copenhagen, Denmark⁹

G. Daskalakis, A. Kyriakis, C. Markou, E. Simopoulou, I. Siotis, A. Vayaki

Nuclear Research Center Demokritos (NRCD), Athens, Greece

A. Blondel, G. Bonneaud, J.-C. Brient, P. Bourdon, A. Rougé, M. Rumpf, A. Valassi,⁶ M. Verderi, H. Videau

Laboratoire de Physique Nucléaire et des Hautes Energies, Ecole Polytechnique, IN²P³-CNRS, 91128 Palaiseau Cedex, France

D.J. Candlin, M.I. Parsons

*Department of Physics, University of Edinburgh, Edinburgh EH9 3JZ, United Kingdom*¹⁰

T. Boccali, E. Focardi, G. Parrini, K. Zachariadou

Dipartimento di Fisica, Università di Firenze, INFN Sezione di Firenze, 50125 Firenze, Italy

M. Corden, C. Georgiopoulos, D.E. Jaffe

Supercomputer Computations Research Institute, Florida State University, Tallahassee, FL 32306-4052, USA^{13,14}

A. Antonelli, G. Bencivenni, G. Bologna,⁴ F. Bossi, P. Campana, G. Capon, V. Chiarella, G. Felici, P. Laurelli, G. Mannocchi,⁵ F. Murtas, G.P. Murtas, L. Passalacqua, M. Pepe-Altarelli

Laboratori Nazionali dell'INFN (LNF-INFN), 00044 Frascati, Italy

L. Curtis, S.J. Dorris, A.W. Halley, J.G. Lynch, P. Negus, V. O'Shea, C. Raine, J.M. Scarr, K. Smith, P. Teixeira-Dias, A.S. Thompson, E. Thomson, F. Thomson

*Department of Physics and Astronomy, University of Glasgow, Glasgow G12 8QQ, United Kingdom*¹⁰

O. Buchmüller, S. Dhamotharan, C. Geweniger, G. Graefe, P. Hanke, G. Hansper, V. Hepp, E.E. Kluge, A. Putzer, J. Sommer, K. Tittel, S. Werner, M. Wunsch

*Institut für Hochenergiephysik, Universität Heidelberg, 69120 Heidelberg, Fed. Rep. of Germany*¹⁶

R. Beuselinck, D.M. Binnie, W. Cameron, P.J. Dornan, M. Girone, S. Goodsir, E.B. Martin, A. Moutoussi, J. Nash, J.K. Sedgbeer, P. Spagnolo, M.D. Williams

*Department of Physics, Imperial College, London SW7 2BZ, United Kingdom*¹⁰

V.M. Ghete, P. Girtler, E. Kneringer, D. Kuhn, G. Rudolph

*Institut für Experimentalphysik, Universität Innsbruck, 6020 Innsbruck, Austria*¹⁸

A.P. Betteridge, C.K. Bowdery, P.G. Buck, P. Colrain, G. Crawford, A.J. Finch, F. Foster, G. Hughes, R.W.L. Jones, M.I. Williams

*Department of Physics, University of Lancaster, Lancaster LA1 4YB, United Kingdom*¹⁰

I. Giehl, A.M. Greene, C. Hoffmann, K. Jakobs, K. Kleinknecht, G. Quast, B. Renk, E. Rohne, H.-G. Sander, P. van Gemmeren, C. Zeitnitz

*Institut für Physik, Universität Mainz, 55099 Mainz, Fed. Rep. of Germany*¹⁶

J.J. Aubert, C. Benchouk, A. Bonissent, G. Bujosa, J. Carr, P. Coyle, C. Diaconu, F. Etienne, O. Leroy, F. Motsch, P. Payre, M. Talby, A. Sadouki, M. Thulasidas, K. Trabelsi

Centre de Physique des Particules, Faculté des Sciences de Luminy, IN²P³-CNRS, 13288 Marseille, France

M. Aleppo, M. Antonelli, F. Ragusa

Dipartimento di Fisica, Università di Milano e INFN Sezione di Milano, 20133 Milano, Italy

R. Berlich, W. Blum, V. Büscher, H. Dietl, G. Ganis, C. Gotzhein, H. Kroha, G. Lütjens, G. Lutz, C. Mannert, W. Männer, H.-G. Moser, R. Richter, A. Rosado-Schlosser, S. Schael

R. Settles, H. Seywerd, H. Stenzel, W. Wiedenmann, G. Wolf

*Max-Planck-Institut für Physik, Werner-Heisenberg-Institut, 80805 München, Fed. Rep. of Germany*¹⁶

J. Boucrot, O. Callot,² S. Chen, Y. Choi,²¹ A. Cordier, M. Davier, L. Duflot, J.-F. Grivaz, Ph. Heusse, A. Höcker, A. Jacholkowska, D.W. Kim,¹² F. Le Diberder, J. Lefrançois, A.-M. Lutz, I. Nikolic, M.-H. Schune, E. Tournefier, J.-J. Veillet, I. Videau, D. Zerwas

Laboratoire de l'Accélérateur Linéaire, Université de Paris-Sud, IN²P³-CNRS, 91405 Orsay Cedex, France

P. Azzurri, G. Bagliesi,² G. Batignani, S. Bettarini, C. Bozzi, G. Calderini, M. Carpinelli, M.A. Ciocci, R. Dell'Orso, R. Fantechi, I. Ferrante, L. Foà,¹ F. Forti, A. Giassi, M.A. Giorgi, A. Gregorio, F. Ligabue, A. Lusiani, P.S. Marrocchesi, A. Messineo, F. Palla, G. Rizzo, G. Sanguinetti, A. Sciabà, J. Steinberger, R. Tenchini, G. Tonelli,¹⁹ C. Vannini, A. Venturi, P.G. Verdini

Dipartimento di Fisica dell'Università, INFN Sezione di Pisa, e Scuola Normale Superiore, 56010 Pisa, Italy

G.A. Blair, L.M. Bryant, J.T. Chambers, M.G. Green, T. Medcalf, P. Perrodo, J.A. Strong, J.H. von Wimmersperg-Toeller

*Department of Physics, Royal Holloway & Bedford New College, University of London, Surrey TW20 OEX, United Kingdom*¹⁰

D.R. Botterill, R.W. Clift, T.R. Edgecock, S. Haywood, P.R. Norton, J.C. Thompson, A.E. Wright

*Particle Physics Dept., Rutherford Appleton Laboratory, Chilton, Didcot, Oxon OX11 0QX, United Kingdom*¹⁰

B. Bloch-Devaux, P. Colas, S. Emery, W. Kozanecki, E. Lançon, M.-C. Lemaire, E. Locci, P. Perez, J. Rander, J.-F. Renardy, A. Roussarie, J.-P. Schuller, J. Schwindling, A. Trabelsi, B. Vallage

*CEA, DAPNIA/Service de Physique des Particules, CE-Saclay, 91191 Gif-sur-Yvette Cedex, France*¹⁷

S.N. Black, J.H. Dann, R.P. Johnson, H.Y. Kim, N. Konstantinidis, A.M. Litke, M.A. McNeil, G. Taylor

*Institute for Particle Physics, University of California at Santa Cruz, Santa Cruz, CA 95064, USA*²²

C.N. Booth, C.A.J. Brew, S. Cartwright, F. Combley, M.S. Kelly, M. Lehto, J. Reeve, L.F. Thompson

*Department of Physics, University of Sheffield, Sheffield S3 7RH, United Kingdom*¹⁰

K. Affholderbach, A. Böhrer, S. Brandt, G. Cowan, C. Grupen, P. Saraiva, L. Smolik, F. Stephan

*Fachbereich Physik, Universität Siegen, 57068 Siegen, Fed. Rep. of Germany*¹⁶

M. Apollonio, L. Bosisio, R. Della Marina, G. Giannini, B. Gobbo, G. Musolino

Dipartimento di Fisica, Università di Trieste e INFN Sezione di Trieste, 34127 Trieste, Italy

J. Rothberg, S. Wasserbaech

Experimental Elementary Particle Physics, University of Washington, WA 98195 Seattle, U.S.A.

S.R. Armstrong, E. Charles, P. Elmer, D.P.S. Ferguson, Y. Gao, S. González, T.C. Greening, O.J. Hayes, H. Hu, S. Jin, P.A. McNamara III, J.M. Nachtman,²⁴ J. Nielsen, W. Orejudos, Y.B. Pan, Y. Saadi, I.J. Scott, J. Walsh, Sau Lan Wu, X. Wu, J.M. Yamartino, G. Zobernig

Department of Physics, University of Wisconsin, Madison, WI 53706, USA¹¹

¹Now at CERN, 1211 Geneva 23, Switzerland.

²Also at CERN, 1211 Geneva 23, Switzerland.

³Also at Dipartimento di Fisica, INFN, Sezione di Catania, Catania, Italy.

⁴Also Istituto di Fisica Generale, Università di Torino, Torino, Italy.

⁵Also Istituto di Cosmo-Geofisica del C.N.R., Torino, Italy.

⁶Supported by the Commission of the European Communities, contract ERBCHBICT941234.

⁷Supported by CICYT, Spain.

⁸Supported by the National Science Foundation of China.

⁹Supported by the Danish Natural Science Research Council.

¹⁰Supported by the UK Particle Physics and Astronomy Research Council.

¹¹Supported by the US Department of Energy, grant DE-FG0295-ER40896.

¹²Permanent address: Kangnung National University, Kangnung, Korea.

¹³Supported by the US Department of Energy, contract DE-FG05-92ER40742.

¹⁴Supported by the US Department of Energy, contract DE-FC05-85ER250000.

¹⁵Permanent address: Universitat de Barcelona, 08208 Barcelona, Spain.

¹⁶Supported by the Bundesministerium für Bildung, Wissenschaft, Forschung und Technologie, Fed. Rep. of Germany.

¹⁷Supported by the Direction des Sciences de la Matière, C.E.A.

¹⁸Supported by Fonds zur Förderung der wissenschaftlichen Forschung, Austria.

¹⁹Also at Istituto di Matematica e Fisica, Università di Sassari, Sassari, Italy.

²⁰Now at Schweizerischer Bankverein, Basel, Switzerland.

²¹Permanent address: Sung Kyun Kwan University, Suwon, Korea.

²²Supported by the US Department of Energy, grant DE-FG03-92ER40689.

²³Now at School of Operations Research and Industrial Engineering, Cornell University, Ithaca, NY 14853-3801, U.S.A.

²⁴Now at University of California at Los Angeles (UCLA), Los Angeles, CA 90024, U.S.A.

1 Introduction

The long-standing discrepancy between theoretical predictions and measurements of the semileptonic branching ratio of heavy hadrons [1] may possibly be solved by calculations including higher-order corrections [2]. However, the puzzle of the different lifetimes of b-mesons and b-baryons remains. The ratio of lifetimes $\tau_{\text{b-baryon}}/\tau_{\text{B}^0}$ is predicted to be not smaller than 0.9 [3] while present measurements yield a value of 0.73 ± 0.08 [4]. Under the assumption that the semileptonic widths of all b-hadrons are the same this ratio can be probed independently by a measurement of the semileptonic branching ratio of b-baryons and mesons. Given the experimental measurements of lifetimes, a significantly smaller semileptonic branching ratio is expected for b-baryons than for b-mesons.

The measurement of the absolute branching ratio $\text{BR}(\text{b-baryon} \rightarrow \text{pl}\bar{\nu}X)$ is presented here.² Its evaluation requires the knowledge of the overall number of b-baryons and hence an estimate is made of the b-baryon fraction f_{Λ_b} , derived from proton production in b-hadron decays. The ratio $R_{\text{pl}} = \text{BR}(\text{b-baryon} \rightarrow \text{pl}\bar{\nu}X)/\text{BR}(\text{b-baryon} \rightarrow \text{p}X)$ is expected to be a good estimator for $\text{BR}(\text{b-baryon} \rightarrow lX)$. This is compared with the overall semileptonic branching ratio $\text{BR}(\text{b} \rightarrow lX)$ which is known more precisely than the corresponding branching ratio of any specific b-hadron state.

For the evaluation of f_{Λ_b} , b events are selected with help of a b-tag algorithm and protons are statistically identified by their specific energy loss in the detector. The main difficulty is to distinguish protons produced in b-hadron decay from those from fragmentation. The method used here is based on the impact parameter of the tracks and their angle with respect to the thrust axis. The two variables are independent and display good separation power between leading and non-leading particles.

In parallel to the search for protons from b decays, charged particle production is studied in $Z \rightarrow \text{b}\bar{\text{b}}$, $Z \rightarrow \text{c}\bar{\text{c}}$ and $Z \rightarrow \text{u}\bar{\text{u}}, \text{d}\bar{\text{d}}, \text{s}\bar{\text{s}}$ events separately. The momentum spectra are measured for pions, kaons and protons and the corresponding mean multiplicities are calculated. These measurements are important to shed more light on the fragmentation of quarks and gluons into hadrons. At the same time the measurement of the rates and momentum spectra of particles produced in b-hadron decays helps to assure a correct description of the weak decay of b-hadrons in the Monte Carlo simulation.

The following sections describe the detector and its performance, event and track selection, particle identification with dE/dx , the selection of b decay particles, proton-lepton correlations and the systematic uncertainties of the analysis. Conclusions summarizing the results are given at the end of the paper.

²Charge conjugated modes are always included if not stated otherwise.

2 The detector

The ALEPH detector is described in detail elsewhere [5, 6] and only a brief overview of the most relevant parts for this analysis is given here.

The momentum of charged particles is measured in three concentric tracking chambers. The innermost is the vertex detector consisting of two layers of double sided silicon microstrips with radii of 6.5 cm and 11.3 cm, respectively. The spatial resolution for the $r\phi$ and z projections is $12\ \mu\text{m}$ at normal incidence. The vertex detector is surrounded by the inner drift chamber (ITC) with eight coaxial wire layers. Outside the ITC the time projection chamber (TPC) provides up to 21 three-dimensional space points per track. The TPC has inner and outer radii of 30 and 180 cm and is 2.2 m long. The three tracking detectors are placed within a superconducting solenoid providing a magnetic field of 1.5 T, and together give a transverse momentum resolution of $\sigma(p)/p = 6 \times 10^{-4} p$ for high momentum tracks (p in GeV/ c). The TPC also provides up to 338 measurements of the ionization loss of a track and is essential for the identification of charged particles. The specific energy loss dE/dx is estimated from the truncated mean of the usable samples associated with a track, discarding the lower 8% and upper 40% of the samples. For an electron with the full complement of measurements at a polar angle of $\Theta = 45^\circ$ a resolution of 4.5% is achieved. About 88% of all tracks have at least 50 dE/dx samples. A more detailed description of the ALEPH dE/dx measurement can be found in [6] and [7].

The TPC is surrounded by a lead/proportional-chamber electromagnetic calorimeter segmented into $0.9^\circ \times 0.9^\circ$ projective towers and read out in three sections in depth with an energy resolution of $\sigma(E)/E = 0.18/\sqrt{E} + 0.009$ (E in GeV). In the electromagnetic calorimeter electrons and photons can be identified by their characteristic longitudinal and transverse shower developments. The iron return yoke of the magnet is instrumented with streamer tubes to form a hadron calorimeter and is surrounded by two additional double layers of streamer tubes to aid in muon identification.

The interaction point is reconstructed on an event-by-event basis using the constraint of the average beam spot position [6] resulting in an average resolution of $85\ \mu\text{m}$ for $Z \rightarrow b\bar{b}$ events, projected along the sphericity axis of the event.

3 Event and track selection

The data used in this analysis were recorded by the ALEPH detector during the years 1992–1994. The selection of hadronic events is based on charged tracks and is described elsewhere [8]. Only events with a thrust axis fulfilling $|\cos\theta_{thrust}| < 0.85$ are taken into account leading to about 2.3 million selected hadronic Z decays. Further cuts are applied on the quality of the tracks in these events. Each track must have at least four measured points in the TPC and at

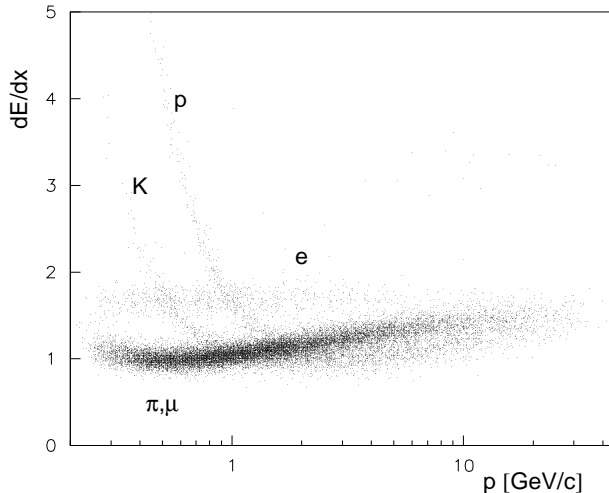


Figure 1: *The mean dE/dx of a sample of 20 000 tracks as a function of their momentum. The energy loss of minimal ionizing particles is normalized to one.*

least 125 single dE/dx measurements. The tracks must originate from within a cylinder of radius 2 cm and length 20 cm centred on the nominal interaction point. The polar angle of the tracks must satisfy $|\cos \theta_{track}| < 0.85$ and a minimum momentum of 300 MeV/ c is required. To avoid protons from interactions with the detector material only negatively charged tracks are selected for momenta lower than 3 GeV/ c .

4 Particle identification

Charged particles are identified by their specific energy loss in the TPC. Figure 1 shows the truncated mean dE/dx as a function of the momentum for selected tracks from hadronic events. The number of pions, kaons and protons are obtained from the tracks' dE/dx distribution by means of an extended maximum likelihood fit. The probability density for a given particle with a measured energy loss dE/dx under the particle hypothesis $j = \pi, K, p, e, \mu$ has been parametrized in a similar way to [7] but for this analysis a ‘bifurcated’ Gaussian has been used to allow a better description of the asymmetric tails of the dE/dx distribution:

$$G^j(dE/dx) = \frac{2}{\sqrt{2\pi}(\sigma_+ + \sigma_-)} \exp\left(-\frac{(dE/dx - \langle dE/dx \rangle_{\text{exp}}^j)^2}{2\sigma_{\pm}^2}\right), \quad (1)$$

with $\sigma_{\pm} = \sigma_-$ for $dE/dx < \langle dE/dx \rangle_{\text{exp}}^j$ and $\sigma_{\pm} = \sigma_+$ for $dE/dx \geq \langle dE/dx \rangle_{\text{exp}}^j$, while $\langle dE/dx \rangle_{\text{exp}}^j$ stands for the expected energy loss under the particle hypothesis j . The σ_+ and σ_- are parametrized as

$$\sigma_+ / \langle dE/dx \rangle_{\text{exp}} = A\sigma_- / \langle dE/dx \rangle_{\text{exp}} = \sigma_0 n_s^{p_1} l^{p_2} (\langle dE/dx \rangle_{\text{exp}})^{p_3}, \quad (2)$$

with A being a free parameter in the likelihood fit (which in general is found to be close to one). Here, n_s is the number of single dE/dx measurements, and l is the normalized mean sample length per measurement. The exponents p are expected to be close to 0.5 [9]. Together with σ_0 they were determined to be $p_1 = -0.5$, $p_2 = p_3 = -0.4$ and $\sigma_0 = 0.82$ from identified, low momentum particles [6]. The expected energy loss per unit length $\langle dE/dx \rangle_{\text{exp}}^j$ is given by the Bethe-Bloch formula [10], a parametrization of which was fit to the ALEPH data from all particles in the low β region and from pions at higher momenta. Muons are not distinguished in the fit as their fraction is small with respect to the pions and hence it is fixed to the Monte Carlo prediction. The introduced uncertainties, mainly on the pion rates, are minor.

For the complete likelihood, the probability density is first summed over all possible particle types weighted with the corresponding particle fractions f_j (which are – together with A – the free parameters in the likelihood fit). Then the probabilities of all tracks are multiplied:

$$\mathcal{L} = \frac{e^{-\phi} \phi^N}{N!} \prod_{i=1}^N \left(\sum_j f_j G_i^j(dE/dx^i, \langle dE/dx \rangle_{\text{exp}}^j, \sigma_{ji}) \right). \quad (3)$$

The Poisson factor in front represents the probability of obtaining a sample of size N from a distribution of mean ϕ , where ϕ is an additional free parameter in the fit. The sum of the particle fractions is constrained to one.

Some examples of the likelihood fit results are shown in Fig. 2 to illustrate the quality.

5 π , K and proton production

5.1 Decomposition of the track samples

All selected events are divided into two hemispheres, defined by the plane perpendicular to the thrust axis. On each hemisphere a b-tag is applied giving the probability for this hemisphere to contain only tracks from the primary vertex. The performance of the b-tag is described in detail in [11]. Five intervals of the b-tag variable are defined and all tracks are assigned to one of these intervals according to the b-tag result of the opposite hemisphere in the same event. (The opposite hemisphere is used to minimize a possible bias introduced by the b-tag.) Using the tracks in each subsample the likelihood fit gives the number of pion, kaons and protons for 50 different momentum bins. The composition of the particles regarding their origin can be described for each of the five samples i by:

$$N_j^i = \epsilon_b^i N_j^b + \epsilon_c^i N_j^c + \epsilon_{\text{uds}}^i N_j^{\text{uds}} \quad j = \pi, K, p; i = 1 \dots 5, \quad (4)$$

where N_j^b , N_j^c and N_j^{uds} are the (unknown) number of pions, kaons or protons in b, c, and uds hemispheres and ϵ_b^i , ϵ_c^i and ϵ_{uds}^i are the fractions of b, c and uds

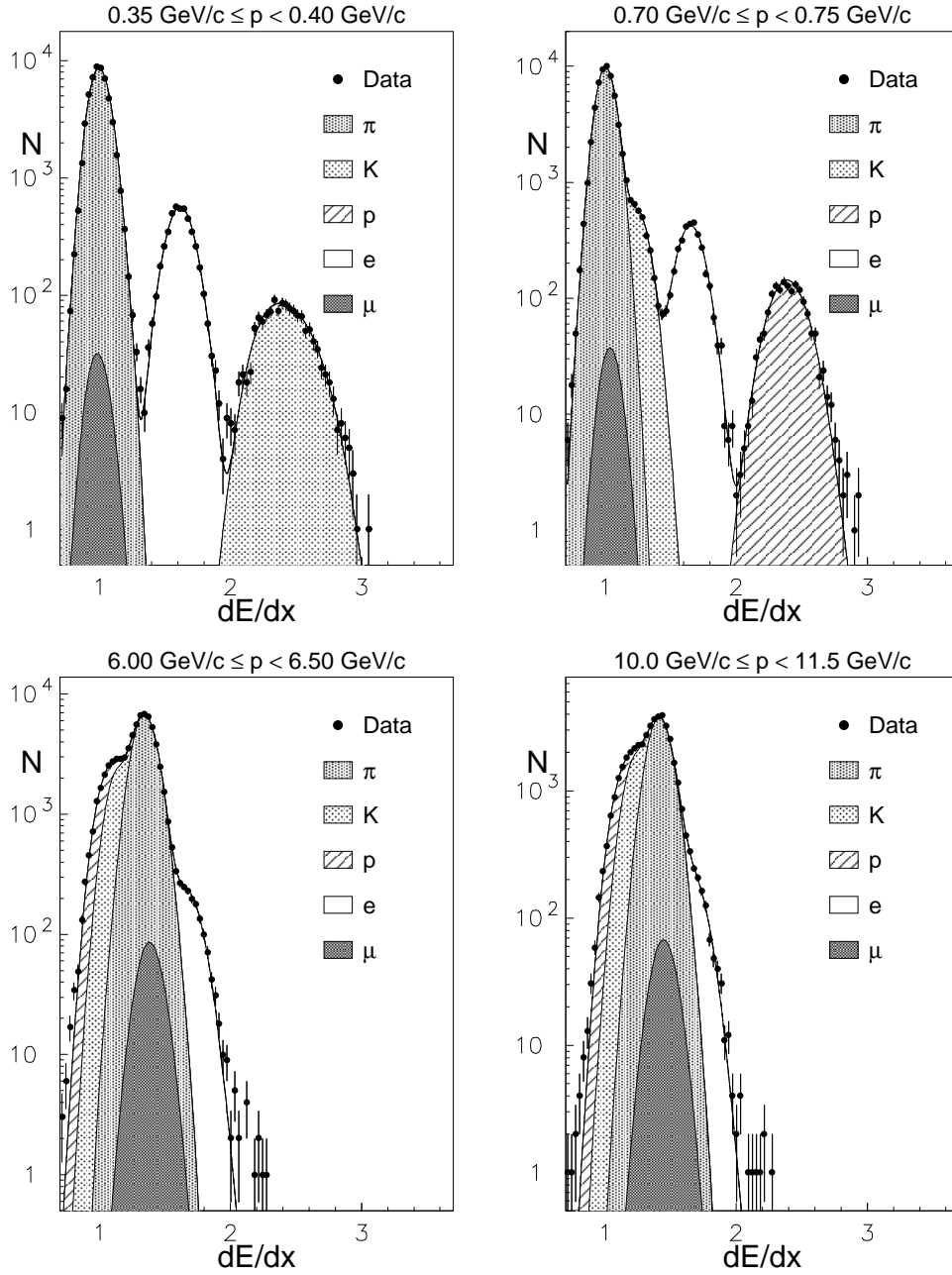


Figure 2: Specific energy loss of selected particles together with the likelihood fit result in different momentum bins. The full dots represent the data, the hatched regions indicate the different particle fractions and the line is the overall fit function.

hemispheres which fall in the b-tag interval i . Almost all the fractions ϵ^i can be derived from data following closely the method described in [11]. To do this the number of hemispheres N^{H^i} , within a specific b-tag interval i , can be written as

$$N^{H^i} = (\epsilon_b^i R_b + \epsilon_c^i R_c + \epsilon_{uds}^i R_{uds}) N_{\text{tot}}^H, \quad (5)$$

with N_{tot}^H being the total number of hemispheres, R_b the ratio of partial widths $\Gamma_{Z \rightarrow b\bar{b}}/\Gamma_{Z \rightarrow \text{hadrons}}$ and with R_c and R_{uds} being defined analogously to R_b . The number of events with both hemispheres in the same interval i is then given by

$$N^{E^i} = (\epsilon_b^{D^i} R_b + \epsilon_c^{D^i} R_c + \epsilon_{uds}^{D^i} R_{uds}) N_{\text{tot}}^E, \quad (6)$$

with $\epsilon^{D^i} = \lambda^i \epsilon^{i^2}$ taking account of the correlation between the two hemispheres (of the order of 10%) by means of the factors λ^i . The λ^i values are taken from simulations. With the partial decay widths of the Z fixed to their Standard Model predictions and the constraint $\sum_i \epsilon_{\text{flav}}^i = 1$ almost all fractions can be calculated from data. Only the three least significant (of fifteen) are fixed to their Monte Carlo predictions.

The number of pions, kaons and protons in $Z \rightarrow b\bar{b}$, $Z \rightarrow c\bar{c}$ and $Z \rightarrow u\bar{u}, d\bar{d}, s\bar{s}$ ($N_j^b, N_j^c, N_j^{\text{uds}}$) is calculated from Eq. 4 for each momentum bin. The resulting momentum spectra are given in Fig. 7 to 9. They have been corrected for the effects of geometrical acceptance, track reconstruction efficiency and interactions in the material of the detector, using an event generator based on the DYMU [12] and JETSET 7.3 [13] programs, in which the decay properties of heavy flavour hadrons were significantly extended. The spectra are normalized to the number of hadronic Z decays and are the weighted mean of the three years of data taking. The expectations of the Monte Carlo, which was tuned to reproduce global event shape and charged particle inclusive distributions [14], are indicated by the overlaid curves. The ‘holes’ in the spectra correspond to those momentum regions where the dE/dx distributions of different particle types overlap so heavily that the fit is no longer sensitive to those particle fractions. These regions were excluded from the analysis. In the appendix the spectra are given in tabular form, a computer readable form can be found at [15].

To measure the number of particles from b-hadron decays the track samples are further classified. Within each of the five b-tag intervals the tracks are divided into four classes: tracks with positive impact parameter, tracks with negative impact parameter, tracks with $|\cos \alpha| > 0.975$, where α is the angle between track and thrust axis, and tracks with $|\cos \alpha| < 0.975$. This leads to 20 different samples and hence to 20 equations per particle type, describing the particle composition. In the following the index j is omitted for simplicity:

$$\begin{aligned} N^{i,\text{class}} &= \epsilon_b^i (\epsilon_{\text{bdecay}}^{\text{class}} N_{\text{bdecay}}^b + \epsilon_{\text{accomp}}^{\text{class}} N_{\text{accomp}}^b) \\ &+ \epsilon_c^i \epsilon_c^{\text{class}} N^c \\ &+ \epsilon_{uds}^i \epsilon_{uds}^{\text{class}} N^{\text{uds}}, \end{aligned} \quad (7)$$

Monte Carlo

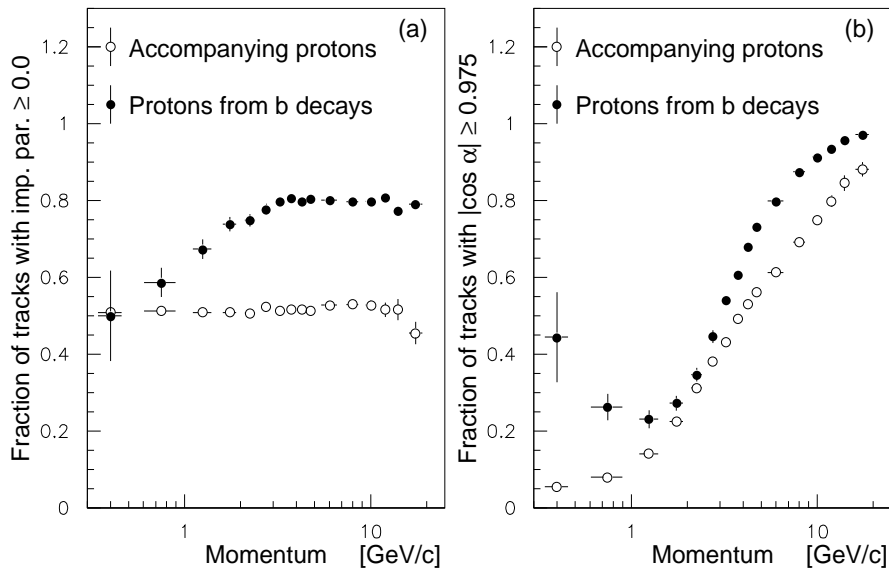


Figure 3: (a) the fraction of protons with positive impact parameter depending on origin and momentum of the particle as predicted from Monte Carlo simulations of b-hadron decays. (b) the same for the fraction of protons with $|\cos \alpha| > 0.975$.

where $N^{i,\text{class}}$ is the overall number of particles in the b-tag interval i fulfilling requirement ‘class’ (positive/negative impact parameter, $|\cos \alpha| < 0.975/ > 0.975$) and $N_{\text{bdecay}}^{\text{b}}$, $N_{\text{accomp}}^{\text{b}}$, N^{c} and N^{uds} are the number of particles from b decays, accompanying the b-hadron in b events, and the number in c events and uds events. The fraction of particles from b decays satisfying the criteria ‘class’ is indicated by $\epsilon_{\text{bdecay}}^{\text{class}}$, while $\epsilon_{\text{accomp}}^{\text{class}}$, $\epsilon_{\text{uds}}^{\text{class}}$ and $\epsilon_{\text{c}}^{\text{class}}$ are defined analogously. All these fractions are taken from Monte Carlo simulations. Then $N_{\text{bdecay}}^{\text{b}}$ and $N_{\text{accomp}}^{\text{b}}$ can be calculated from Eqs. 4 and 7 if the difference between $\epsilon_{\text{bdecay}}^{\text{class}}$ and $\epsilon_{\text{accomp}}^{\text{class}}$ is sizeable. The separation power of the two variables is shown in Fig. 3. In Fig. 3 (a) the fractions of protons with positive impact parameter are given for b-hadron decays and accompanying the b-hadron. Figure 3 (b) shows the discrimination on the basis of $|\cos \alpha| > 0.975$.

After performing the likelihood fit for each sample the numbers of pions, kaons and protons from b-hadron decays and accompanying the b-hadrons are calculated from Eq. 7 for all momentum bins. The resulting spectra are shown in Fig. 10 and 11. Below 1 GeV/c the small number of protons from b decays is not accessible because of the high background from fragmentation protons.

5.2 Multiplicities

The momentum spectra of pions, kaons and protons in $Z \rightarrow b\bar{b}$, $Z \rightarrow c\bar{c}$, $Z \rightarrow u\bar{u}, d\bar{d}, s\bar{s}$ events, in b-hadron decays and accompanying the b-hadron in b events are shown in Figs. 7 to 11. After extrapolating the spectra with help of the simulation over the full kinematic range the corresponding mean multiplicities can be calculated. They are given in tables 1 to 3.

origin	π^\pm			
$Z \rightarrow q\bar{q}$	17.04	\pm	0.005 _{stat}	\pm 0.31 _{sys}
$Z \rightarrow uds$	16.86	\pm	0.02 _{stat}	\pm 0.52 _{sys}
$Z \rightarrow c\bar{c}$	15.93	\pm	0.07 _{stat}	\pm 1.31 _{sys}
$Z \rightarrow b\bar{b}$	18.44	\pm	0.03 _{stat}	\pm 0.63 _{sys}
b decay	3.97	\pm	0.02 _{stat}	\pm 0.21 _{sys}

Table 1: *Pion multiplicities in Z and b-hadron decays*

origin	K^\pm			
$Z \rightarrow q\bar{q}$	2.26	\pm	0.002 _{stat}	\pm 0.12 _{sys}
$Z \rightarrow uds$	2.14	\pm	0.008 _{stat}	\pm 0.13 _{sys}
$Z \rightarrow c\bar{c}$	2.44	\pm	0.03 _{stat}	\pm 0.23 _{sys}
$Z \rightarrow b\bar{b}$	2.63	\pm	0.008 _{stat}	\pm 0.14 _{sys}
b decay	0.72	\pm	0.020 _{stat}	\pm 0.06 _{sys}

Table 2: *Kaon multiplicities in Z and b-hadron decays*

origin	p, \bar{p}			
$Z \rightarrow q\bar{q}$	1.00	\pm	0.002 _{stat}	\pm 0.07 _{sys}
$Z \rightarrow uds$	1.04	\pm	0.006 _{stat}	\pm 0.07 _{sys}
$Z \rightarrow c\bar{c}$	0.87	\pm	0.02 _{stat}	\pm 0.10 _{sys}
$Z \rightarrow b\bar{b}$	1.00	\pm	0.007 _{stat}	\pm 0.08 _{sys}
b decay	0.131	\pm	0.004 _{stat}	\pm 0.011 _{sys}

Table 3: *Proton multiplicities in Z and b-hadron decays*

A comparison with results from other e^+e^- experiments can be found in tables 4, 5 and 6. In all cases the agreement is very good. The proton production in b-hadron decays as measured at LEP is found to differ significantly from the $\Upsilon(4S)$ value. This is due to b-baryon production on the Z resonance.

Mean multiplicities in $Z \rightarrow q\bar{q}$			
	this analysis	DELPHI	OPAL
π^\pm	17.04 ± 0.31	—	17.05 ± 0.43
K^\pm	2.26 ± 0.12	2.26 ± 0.18	2.42 ± 0.13
p, \bar{p}	1.00 ± 0.07	1.07 ± 0.14	0.92 ± 0.11

Table 4: Mean multiplicity of different particles in comparison with DELPHI [16] and OPAL [17].

Mean multiplicities in $Z \rightarrow b\bar{b}$		
	this analysis	DELPHI
π^\pm	18.44 ± 0.63	—
K^\pm	2.63 ± 0.14	2.74 ± 0.50
p, \bar{p}	1.00 ± 0.08	1.13 ± 0.27

Table 5: Mean multiplicities of different particles in $Z \rightarrow b\bar{b}$ in comparison with DELPHI results [18].

Mean multiplicities in b-hadron decays			
	this analysis	DELPHI	ARGUS/CLEO
π^\pm	3.97 ± 0.21	—	4.11 ± 0.08
K^\pm	0.72 ± 0.06	0.88 ± 0.19	0.78 ± 0.03
p, \bar{p}	0.131 ± 0.011	0.141 ± 0.059	0.08 ± 0.004

Table 6: Mean multiplicities of pions, kaons and protons in b-hadron decays in comparison to DELPHI measurements [18] and to measurements by ARGUS and CLEO in $\Upsilon(4S)$ decays [4]. In contrast to Z decays only B^\pm and B^0 are produced there, leading to a significant lower proton production from b decays.

Adding the lepton multiplicity in b decays from $\text{Br}(b \rightarrow lX)$, $\text{Br}(b \rightarrow c \rightarrow lX)$ [19] and $\text{Br}(b \rightarrow c\bar{c}s \rightarrow lX)$ [20] to the multiplicities of pions, kaons and protons in table 6 the mean multiplicity of charged hadrons in b decays is found to be

$$\langle n_b \rangle = 5.24 \pm 0.25 . \quad (8)$$

The result is dominated by systematics and can be compared with measurements of DELPHI [18] and OPAL [21] which gave $\langle n_b \rangle = 5.84 \pm 0.38$ and 5.51 ± 0.51 , respectively.

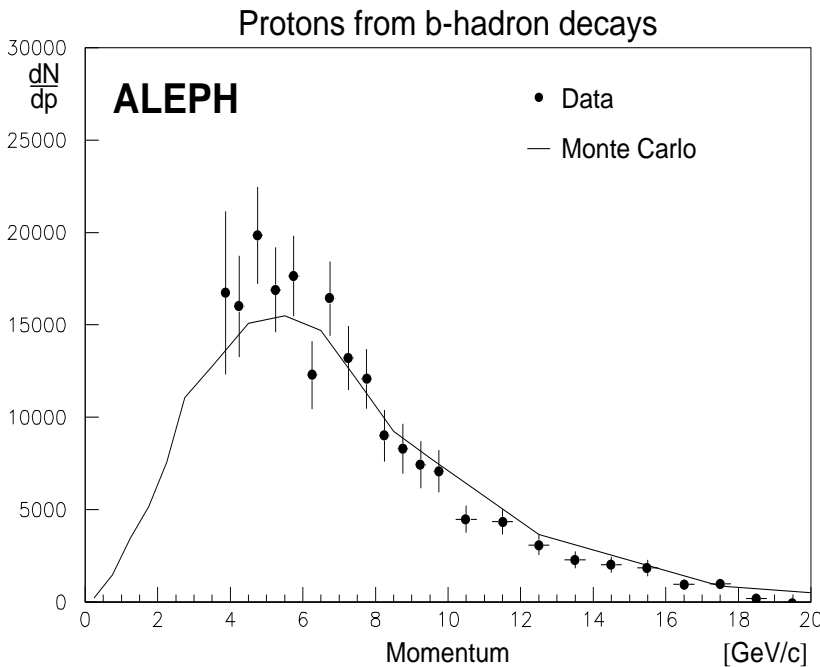


Figure 4: *Momentum spectra for protons from b decays: data and Monte Carlo prediction. The Monte Carlo is normalized to the data.*

5.3 The b-baryon fraction f_{Λ_b}

The overall number of protons from b-hadron decay is used to estimate the b-baryon fraction f_{Λ_b} . Assuming that $\text{BR}(\text{b-baryon} \rightarrow \text{p}X)$ is considerably larger than $\text{BR}(\text{b-meson} \rightarrow \text{p}X)$ even a small fraction of b-baryons will lead to a sizeable increase of protons in b-hadron decays with respect to the pure meson sample, as e.g. in $\Upsilon(4S)$ decays.

The number of protons from b-hadron decays N_p is related to the b-baryon fraction as follows

$$N_p = (f_{\Lambda_b} \text{BR}(\text{b-baryon} \rightarrow \text{p}X) + (1 - f_{\Lambda_b}) \text{BR}(\text{b-meson} \rightarrow \text{p}X)) N_b \quad (9)$$

with the number of b-hadron decays N_b being calculated from the overall number of events multiplied by $2R_b$ (using the Standard Model value for R_b). The equation can be solved for f_{Λ_b}

$$f_{\Lambda_b} = \frac{N_p/N_b - \text{BR}(\text{b-meson} \rightarrow \text{p}X)}{\text{BR}(\text{b-baryon} \rightarrow \text{p}X) - \text{BR}(\text{b-meson} \rightarrow \text{p}X)}. \quad (10)$$

To extract N_p the measured momentum spectra of b decay protons is extrapolated from 3.75 GeV/c to zero using the Monte Carlo prediction as indicated in Fig. 4. The branching ratio $\text{BR}(\text{B}^\pm, \text{B}^0 \rightarrow \text{p}X)$ has been measured at the $\Upsilon(4S)$ by ARGUS and CLEO to be $(8.0 \pm 0.4)\%$ [4] but $\text{BR}(\text{B}_s \rightarrow \text{p}X)$ is unknown. As a conservative estimate $\text{BR}(\text{B}_s \rightarrow \text{p}X) = (8.0 \pm 4.0)\%$ has been assumed. The B_s fraction in b events was taken from [4].

Because no measurements are available for $\text{BR}(\text{b-baryon} \rightarrow \text{p}X)$ it has to be estimated. Naively $\text{BR}(\text{b-baryon} \rightarrow \text{p}X)$ is close to $\text{BR}(\text{b-baryon} \rightarrow \text{n}X)$ and hence about 50%. But this assumption does not fully hold true, taking e.g. isospin arguments and the decay via Λ or Σ particles into account which lead to different branching ratios into protons and neutrons. As an upper limit it has been assumed that all b-baryon decays produce a Λ and therefore $\text{BR}(\text{b-baryon} \rightarrow \text{p}X) = 64\%$. For a lower estimate $\text{BR}(\text{b-baryon} \rightarrow \Lambda X) = \text{BR}(\text{b-baryon} \rightarrow \Sigma^+ X) = \text{BR}(\text{b-baryon} \rightarrow \Sigma^0 X) = \text{BR}(\text{b-baryon} \rightarrow \Sigma^- X) = 25\%$ has been assumed. This results in $\text{BR}(\text{b-baryon} \rightarrow \text{p}X) = 45\%$. The mean value is $(54.5 \pm 5.5)\%$, the error is taken from the standard deviation of a uniform probability distribution. However there are also b-baryon decays with three baryons in the final state. The branching ratio for these is taken from the Monte Carlo prediction and adds 3% to the above estimate with an assumed relative uncertainty of 50%. Hence $\text{BR}(\text{b-baryon} \rightarrow \text{p}X) = (58 \pm 6)\%$ has been used for the calculation of the b-baryon fraction. The result is

$$f_{\Lambda_b} = (10.2 \pm 0.7_{\text{stat}} \pm 2.2_{\text{sys1}} \pm 1.6_{\text{sys2}})\%. \quad (11)$$

Here the first systematic error represents uncertainties related to the analysis and the second uncertainties related to the branching ratios. The systematic uncertainties of the measurement are discussed in section 7. The resulting baryon fraction can be compared to the value $(13.2 \pm 4.1)\%$ calculated from $\text{BR}(\text{b-baryon} \rightarrow \Lambda_c l \bar{\nu} X)$ and the b-baryon lifetime [4] and is found to be in good agreement.

6 Proton-lepton correlation

For the search for proton-lepton³ pairs from b-baryon decays the analysis is restricted to events containing a high momentum lepton candidate. (The selection of leptons within ALEPH is discussed in [19] and [22].) For this analysis only tracks with opposite charge with respect to the lepton candidate are selected and the angle between the track and the thrust axis is not used because of possible correlations with the transverse momentum of the lepton. The selection cuts for the tracks are slightly released to gain efficiency and no b-tag is performed. The presence of a high momentum lepton candidate sufficiently enriches the event sample with b events.

The impact parameter of the proton candidates is again used to measure their number in b decays while the p_T of the lepton with respect to the jet axis is used to identify the proton-lepton pairs from b-baryons and distinguish them from background processes. Possible background sources for proton-lepton pairs are listed below:

³'lepton' stands for electron or muon

Composition of the proton-lepton pair sample	
Source	number per b-baryon decay
b-baryon decays	free parameter
$b \rightarrow c\bar{c}s, \bar{c} \rightarrow l\bar{\nu}X$	0.012
$b \rightarrow \tau\bar{\nu}pX, \tau \rightarrow l\bar{\nu}\nu$	0.002
b-meson $\rightarrow \Lambda_c\bar{p}X, \Lambda_c \rightarrow l\bar{\nu}X$	free parameter
b-meson $\rightarrow \bar{p}l\bar{\nu}X$	free parameter
$b \rightarrow pX + \text{fake lepton}$	free parameter

Table 7: *Composition of the proton lepton sample where the protons come from b-hadron decay. As indicated two contributions are fixed within the analysis, the others are left free.*

1. Decay of the b quark into $c\bar{c}s$ with subsequent semileptonic \bar{c} quark decay in l^-X . An example is the decay $\Lambda_b \rightarrow \bar{D}_s pX, \bar{D}_s \rightarrow l^-X$. Using $\text{BR}(b \rightarrow c\bar{c}s, \bar{c} \rightarrow lX) = (1.3 \pm 0.5)\%$ [20] and $\text{BR}(b\text{-baryon} \rightarrow pX) \approx 58\%$ about 0.8% of all b-baryons are expected to contribute to this background. A similar assumption for mesons with $\text{BR}(b\text{-meson} \rightarrow pX) = 8.0\%$ leads to approximately 0.004 background events per b-baryon.
2. b-baryon $\rightarrow p\tau X$ with subsequent leptonic decay of the τ lepton. From the known branching ratio of $b \rightarrow \tau X$ one can conclude that about 0.17% of all b-baryons contribute to this background source.
3. b-meson $\rightarrow \Lambda_c\bar{p}X$ followed by a semileptonic decay of the Λ_c .
4. b-meson $\rightarrow \bar{p}lX$.
5. The lepton is produced in pion or kaon decays, in photon conversion or is a misidentified hadron. In the following these will be called ‘fake leptons’.

All background processes (which are summarized in table 7) show considerably softer lepton p_T spectra than the signal process.

Eight data sets are selected. Four intervals, based on the p_T of the lepton candidate, 0.0 and 0.5 GeV/c, 0.5 and 0.8 GeV/c, 0.8 and 1.2 GeV/c and greater than 1.2 GeV/c are chosen and then each set is divided further into one sample containing tracks with positive impact parameters and one containing tracks with negative impact parameters. The number of protons in each sample can be written as:

$$\begin{aligned}
N_{p_T,+}^{pl} &= \epsilon_b^+ \left(\sum_x \epsilon_{p_T}^x N_{pl}^x \right) + \epsilon_{\text{non-b}}^+ N_{p_T}^{\text{non-b}} \\
N_{p_T,-}^{pl} &= \epsilon_b^- \left(\sum_x \epsilon_{p_T}^x N_{pl}^x \right) + \epsilon_{\text{non-b}}^- N_{p_T}^{\text{non-b}}, \tag{12}
\end{aligned}$$

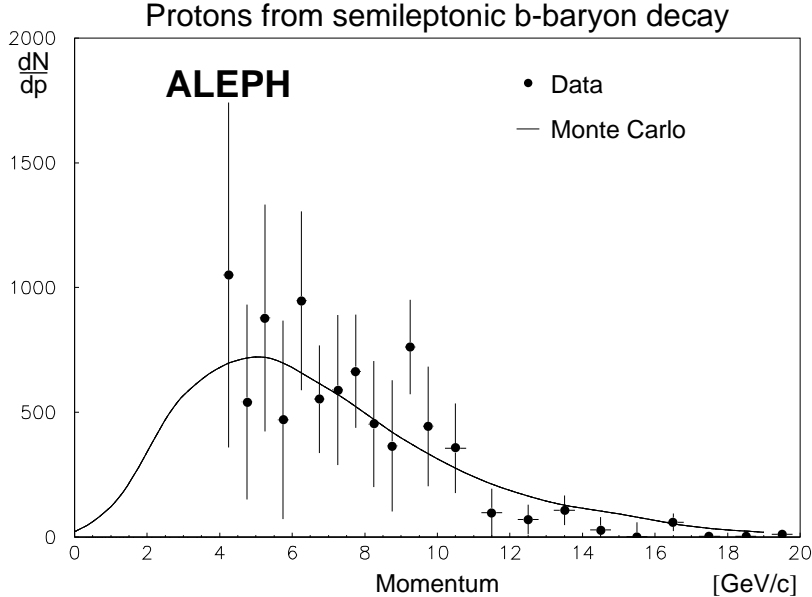


Figure 5: *The momentum spectrum of protons from semileptonic b-baryon decay (electrons and muons). The dots represent the data, the line the Monte Carlo prediction, normalized to the data*

with $N_{p_T,+}^{pl}$ being the measured number of proton-lepton pairs with a transverse momentum of the lepton candidate in the p_T interval \hat{p}_T and a proton with positive impact parameter, $N_{p_T,-}^{pl}$ is defined analogously but contains protons with negative impact parameters. The numbers of proton-lepton pairs from the different sources x (b-baryon decay or one of the background processes described above) are denoted N_{pl}^x and are calculated together with the numbers of proton-lepton pairs $N_{p_T}^{\text{non-b}}$ where the proton does not come from any b decay but the lepton candidate has a p_T in the interval \hat{p}_T . The probability that a lepton from source x has a transverse momentum in the p_T interval \hat{p}_T is written as $\epsilon_{p_T}^x$. These numbers are taken from Monte Carlo. The fraction of protons from b-hadron decays having a positive impact parameter is denoted ϵ_b^+ with $\epsilon_{\text{non-b}}^+$, ϵ_b^- and $\epsilon_{\text{non-b}}^-$ defined analogously. To solve the equations two background contributions are fixed to the expected values given in table 7. The number of protons from b-baryon decays can then be calculated in each momentum bin. The result is given in Fig. 5. Extrapolating the spectrum to zero using Monte Carlo leads to

$$f_{\Lambda_b} \text{BR}(\text{b-baryon} \rightarrow pl\bar{\nu}X) = (4.72 \pm 0.66_{\text{stat}} \pm 0.44_{\text{sys}})10^{-3} . \quad (13)$$

This number is the average of $l = \text{electron}$ and $l = \text{muon}$ and can be compared with a measurement of DELPHI [23]: $f_{\Lambda_b} \text{BR}(\text{b-baryon} \rightarrow p\mu X) = (4.9 \pm 1.1 \pm 1.3)10^{-3}$. Together with f_{Λ_b} from Eq. 11 an absolute branching ratio can be calculated:

$$\text{BR}(\text{b-baryon} \rightarrow pl\bar{\nu}X) = (4.63 \pm 0.72_{\text{stat}} \pm 0.68_{\text{sys1}} \pm 0.71_{\text{sys2}})\% . \quad (14)$$

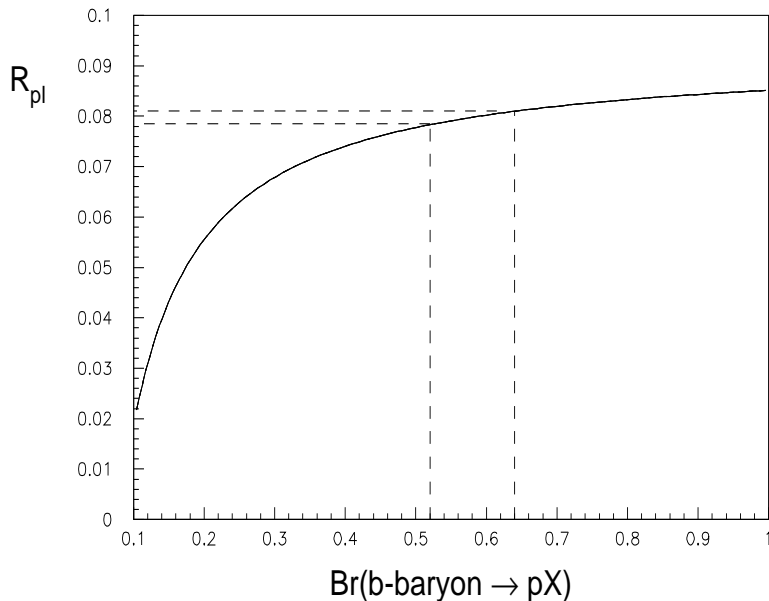


Figure 6: *The dependence of R_{pl} on $BR(b\text{-baryon} \rightarrow pX)$. R_{pl} varies only slightly with $BR(b\text{-baryon} \rightarrow pX)$ over a wide range. Allowing $BR(b\text{-baryon} \rightarrow pX)$ to vary between 0.52 and 0.64, R_{pl} changes only about 0.003. Towards smaller $BR(b\text{-baryon} \rightarrow pX)$ the dependence increases significantly.*

One of the major uncertainties of this result is the estimate of $BR(b\text{-baryon} \rightarrow pX)$. However, the ratio $R_{pl} = BR(b\text{-baryon} \rightarrow pl\bar{\nu}X)/BR(b\text{-baryon} \rightarrow pX)$ is only slightly dependent on this quantity as indicated in Fig. 6. R_{pl} is found to be

$$R_{pl} = \frac{BR(b\text{-baryon} \rightarrow pl\bar{\nu}X)}{BR(b\text{-baryon} \rightarrow pX)} = 0.080 \pm 0.012_{\text{stat}} \pm 0.014_{\text{sys}}. \quad (15)$$

Assuming that

$$\frac{BR(b\text{-baryon} \rightarrow pl\bar{\nu}X)}{BR(b\text{-baryon} \rightarrow lX)} \approx BR(b\text{-baryon} \rightarrow pX) \quad (16)$$

the ratio R_{pl} is close to $BR(b\text{-baryon} \rightarrow lX)$ and can be compared with the recent OPAL measurement [24] of $R_{\Lambda} = 0.070 \pm 0.012 \pm 0.007_{\text{sys}}$, with $R_{\Lambda} = BR(b\text{-baryon} \rightarrow \Lambda l\bar{\nu}X)/BR(b\text{-baryon} \rightarrow \Lambda X)$, which is in very good agreement.

If

$$\frac{\tau_{b\text{-baryon}}}{\tau_b} \approx \frac{BR(b\text{-baryon} \rightarrow lX)}{BR(b \rightarrow lX)} \quad (17)$$

and $R_{pl} \approx BR(b\text{-baryon} \rightarrow lX)$ one can compare the ratio of the semileptonic branching ratios of b-baryons and all b-hadrons

$$\frac{R_{pl}}{BR(b \rightarrow lX)} = 0.72 \pm 0.17 \quad (18)$$

with the corresponding ratio of lifetimes, calculated from [4]:

$$\frac{\tau_{\text{b-baryon}}}{\tau_{\text{b}}} = 0.74 \pm 0.05 . \quad (19)$$

The agreement is again very good. The branching ratio $\text{BR}(\text{b} \rightarrow lX)$ in Z decays has been taken from [4].

7 Systematics

Several sources of systematic uncertainties affect the accuracy of the measurements. They are listed in table 8 and 9 together with the uncertainties due to the limited knowledge of the branching ratios $\text{BR}(\text{b-baryon} \rightarrow \text{p}X)$ and $\text{BR}(\text{b-meson} \rightarrow \text{p}X)$.

The fitted particle rates depend crucially on the expected dE/dx values and resolutions entering the likelihood function. Therefore the expected dE/dx are shifted within the uncertainties of the parametrization of the Bethe-Bloch formula (section 4). The resolution is rescaled and a Gaussian is used instead of a ‘bifurcated’ Gaussian. In the overlap region the added uncertainties are 0.9%, 4% and 6.5% for pions, kaons and protons, respectively. The deviations of subsequent bins are correlated and conservatively all momentum bins within the overlap region are taken as 100 % correlated.

The sign of a track’s impact parameter and its angle with the thrust axis are used to distinguish particles from b-hadron decay from accompanying particles and hence the result relies on the correct simulation of these two quantities. Two checks are performed: First no distinction is made between decay and fragmentation particles. Equation system 7 then reduces to:

$$\begin{aligned} N_{\text{all},i} &= \epsilon_{\text{b}}^i N_{\text{b}} + \epsilon_{\text{c}}^i N_{\text{c}} + \epsilon_{\text{uds}}^i N_{\text{uds}} \\ N_{\text{all},i}^{\text{class}} &= \epsilon_{\text{b}}^{\text{class}} \epsilon_{\text{b}}^i N_{\text{b}} + \epsilon_{\text{c}}^{\text{class}} \epsilon_{\text{c}}^i N_{\text{c}} + \epsilon_{\text{uds}}^{\text{class}} \epsilon_{\text{uds}}^i N_{\text{uds}} . \end{aligned} \quad (20)$$

Here the fractions ϵ^{class} can be measured directly from the data and be compared with the predictions. At very low (high) momentum ϵ^{class} is very close to $\epsilon_{\text{accomp}}^{\text{class}}$ ($\epsilon_{\text{decay}}^{\text{class}}$).

For the second check the number of particles from b-hadron decays are calculated from the positive impact parameter alone and the result is used to calculate the fraction fulfilling $|\cos \alpha| < 0.975$. In both cases the agreement between data and simulation is good and the maximal deviation is taken as the systematic uncertainty.

Attention is given to the numbers of protons coming from long living hyperons such as Λ or Σ . The fraction of protons coming from hyperon decays in b decays has been changed by about 30% in the Monte Carlo to be in agreement with measurements of DELPHI [16] and OPAL [24]. The resulting change in the fraction of protons with positive impact parameter is found to be well covered

Composition of the systematic errors on f_{Λ_b}	
1. Systematic uncertainties from the analysis	
dE/dx	1.7%
b-tag	0.8%
Imp. par. and $\cos\alpha$	0.8%
Extrapolation	0.6%
Reconstr. efficiency	0.5%
Total	2.2%
2. Systematic uncertainties from branching ratios	
BR(b-meson $\rightarrow pX$)	1.0%
BR(b-baryon $\rightarrow pX$)	1.2%
Total	1.6%

Table 8: *The different contributions to the two systematic errors on f_{Λ_b} . The quoted errors are absolute.*

by the systematic uncertainty derived previously. The fraction of tracks from b decays having a positive impact parameter depends on the lifetime of the parent b-hadron. Since one of the motivations of this measurement was to test the difference in lifetimes between b-baryons and b-mesons, the differences found in the impact parameter distribution between Monte Carlo samples with different b lifetimes are taken into account in the systematic uncertainties but are not found to be large.

Several other sources of systematic uncertainties are investigated: the b-tag efficiencies, the reconstruction efficiencies, the muon fraction fixed in the likelihood fit, the efficiency correction of particles from nuclear interactions and the extrapolation of the measured momentum spectra over the whole momentum range. The latter has been checked by using HERWIG 5.6, JETSET 7.3 and JETSET 7.4 for the extrapolation and the JETSET prediction has been compared to the momentum spectra of protons from B^\pm, B^0 decays as measured by ARGUS [25] and CLEO [26] and found to be in good agreement.

Most of the uncertainties discussed above are also present in the proton-lepton analysis and partly cancel in the ratio $(f_{\Lambda_b} \text{BR}(\text{b-baryon} \rightarrow p l \bar{\nu} X))/f_{\Lambda_b}$. Additional uncertainties are due to lepton identification and the simulation of the lepton p_T spectra [19, 22]. The impact of the fixed branching ratios (b $\rightarrow c\bar{c}s$ with semileptonic \bar{c} decay and b-baryon $\rightarrow \tau \bar{\nu} p X$) is small and variations of 50% lead to negligible effects. The modelling of the p_T lepton spectra of the background processes is found to be of minor importance compared to that of the spectrum of the signal leptons. The uncertainty was estimated from the divergence between different theoretical predictions for b-meson decay as described in e.g. [19]. In addition the rate of four body semileptonic b-baryon decays has been varied from 0% to 40% and the Λ_b polarization, as measured by ALEPH in [27], was considered.

Overview over the systematic uncertainties on BR(b-baryon $\rightarrow pl\bar{\nu}X$)	
1. Systematic uncertainties from the analysis	
dE/dx	0.46%
b-tag	0.34%
Impact parameter	0.23%
p_T spectra	0.19%
lepton selection	0.10%
Extrapolation	0.15%
Reconstr. efficiency	0.11%
Total	0.68%
2. Systematic uncertainties from branching ratios	
BR(b-meson $\rightarrow pX$)	0.45%
BR(b-baryon $\rightarrow pX$)	0.55%
Total	0.71%

Table 9: *The different contributions to the two systematic uncertainties on BR(b-baryon $\rightarrow pl\bar{\nu}X$). The errors are absolute.*

The systematic uncertainties on BR(b-baryon $\rightarrow pl\bar{\nu}X$) are listed in table 9.

8 Conclusions

The momentum spectra and mean multiplicities have been measured for pions, kaons and protons in $Z \rightarrow b\bar{b}$, $Z \rightarrow c\bar{c}$ and $Z \rightarrow u\bar{u}, d\bar{d}, s\bar{s}$ separately. In b events particles from b-hadron decay were distinguished from non-leading particles. The b-baryon fraction and the absolute semileptonic branching ratio BR(b-baryon $\rightarrow pl\bar{\nu}X$) have been evaluated from proton production and correlated proton-lepton production in b-hadron decays. The b-baryon fraction was estimated from the overall number of protons from b decays and was found to be

$$f_{\Lambda_b} = (10.2 \pm 0.7_{\text{stat}} \pm 2.7_{\text{sys}})\% . \quad (21)$$

This result was used for the measurement of the absolute branching ratio of the decay b-baryon $\rightarrow pl\bar{\nu}X$.

$$\text{BR}(\text{b-baryon} \rightarrow pl\bar{\nu}X) = (4.63 \pm 0.72_{\text{stat}} \pm 0.98_{\text{sys}})\% . \quad (22)$$

The ratio $R_{pl} = \text{BR}(\text{b-baryon} \rightarrow pl\bar{\nu}X) / \text{BR}(\text{b-baryon} \rightarrow pX)$ has been found to be

$$R_{pl} = 0.080 \pm 0.012_{\text{stat}} \pm 0.014_{\text{sys}} . \quad (23)$$

This relatively small number supports the small lifetime of b-baryons with respect to b-mesons as measured at LEP.

Acknowledgements

We wish to thank our colleagues from the accelerator divisions for the successful operation of the LEP machine, and the engineers and technical staff in all our institutions for their contribution to the good performance of ALEPH. Those of us from non-member states thank CERN for its hospitality.

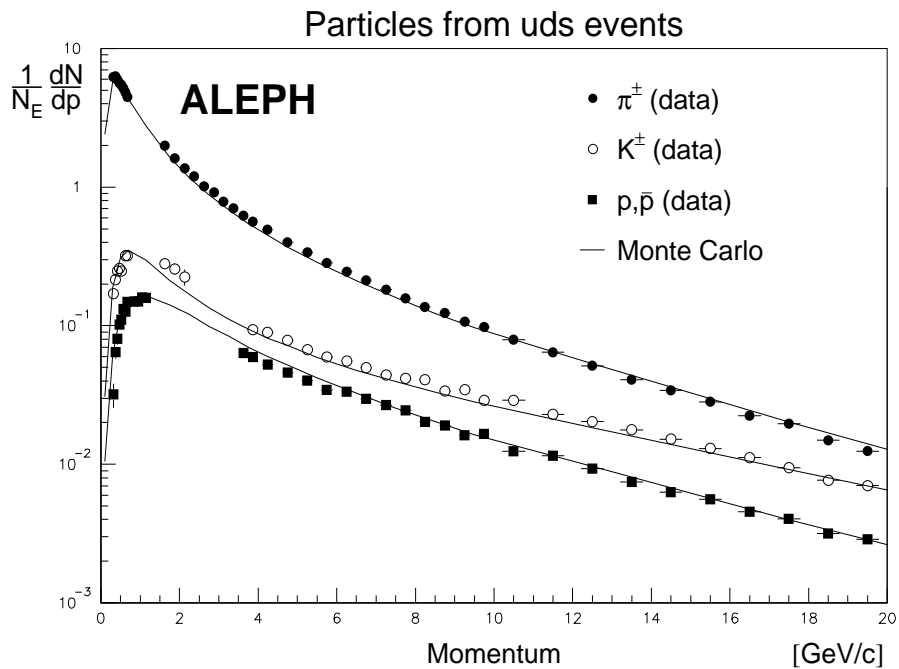


Figure 7: *Momentum spectra from pions, kaons and protons in uds events together with the Monte Carlo predictions. The errors shown are the quadratic sum of statistical and systematic errors.*

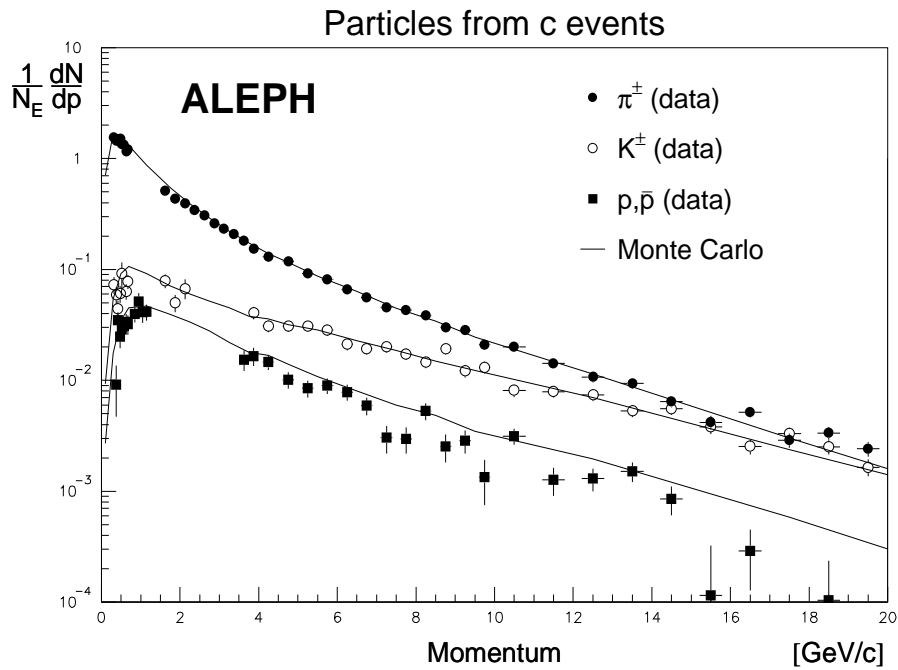


Figure 8: *Momentum spectra from pions, kaons and protons in c events together with the Monte Carlo predictions. The errors shown are the quadratic sum of statistical and systematic errors.*

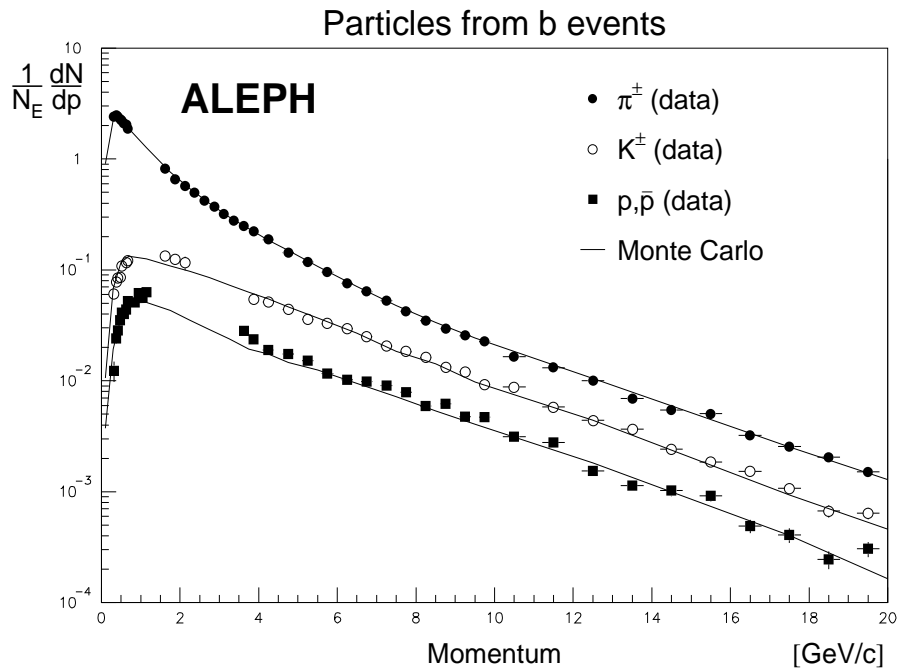


Figure 9: *Momentum spectra from pions, kaons and protons in b events together with the Monte Carlo predictions. The errors shown are the quadratic sum of statistical and systematic errors.*

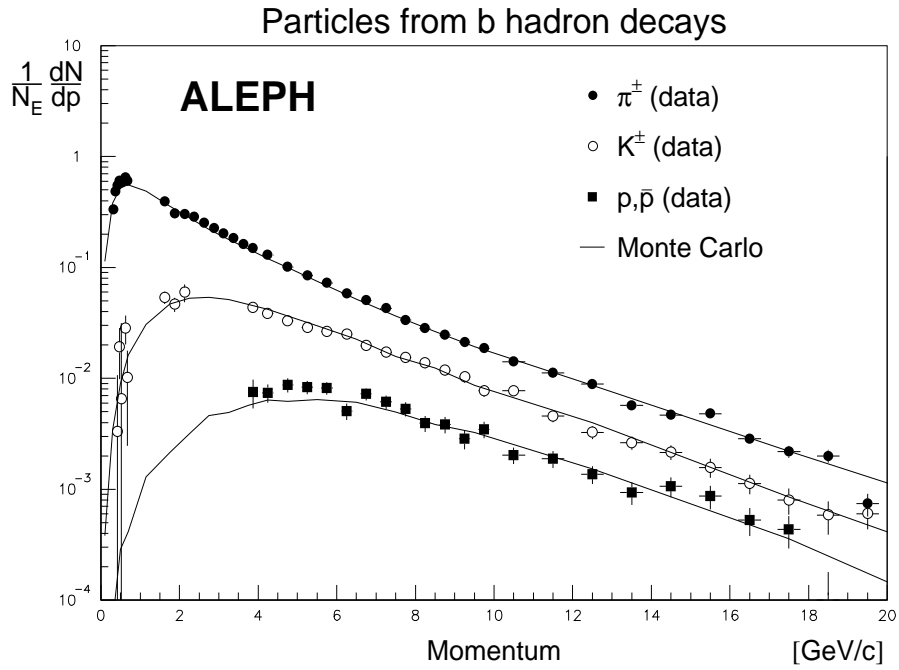


Figure 10: *Momentum spectra from pions, kaons and protons from b-hadron decays together with the Monte Carlo predictions. The errors shown are the quadratic sum of statistical and systematic errors.*

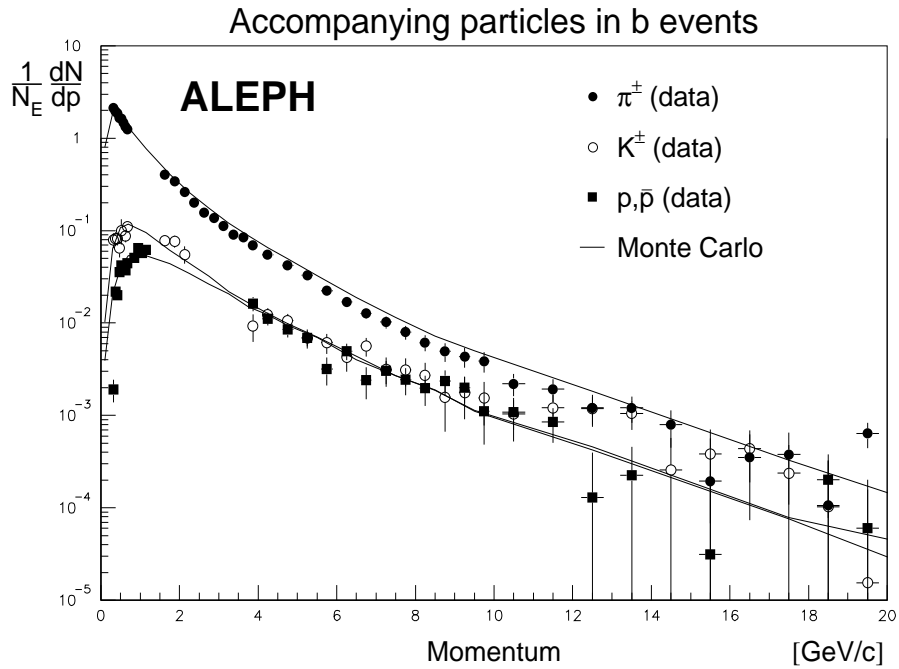


Figure 11: *Momentum spectra of pions, kaons and protons accompanying b-hadrons in b events together with the Monte Carlo predictions. The errors shown are the quadratic sum of statistical and systematic errors.*

Appendix

p interval [GeV/c]	$\frac{1}{N_E} \frac{dN}{dp}$	Δ_{stat}	Δ_{sys}
0.30 – 0.35	6.34 ± 0.04	± 0.19	
0.35 – 0.40	6.33 ± 0.04	± 0.19	
0.40 – 0.45	5.95 ± 0.03	± 0.18	
0.45 – 0.50	5.68 ± 0.03	± 0.18	
0.50 – 0.55	5.47 ± 0.03	± 0.16	
0.55 – 0.60	5.14 ± 0.02	± 0.15	
0.60 – 0.65	4.89 ± 0.02	± 0.15	
0.65 – 0.70	4.49 ± 0.02	± 0.14	
1.50 – 1.75	1.98 ± 0.01	± 0.06	
1.75 – 2.00	1.61 ± 0.01	± 0.05	
2.00 – 2.25	1.36 ± 0.01	± 0.04	
2.25 – 2.50	1.19 ± 0.01	± 0.04	
2.50 – 2.75	1.01 ± 0.01	± 0.03	
2.75 – 3.00	0.906 ± 0.004	± 0.029	
3.00 – 3.25	0.784 ± 0.003	± 0.025	
3.25 – 3.50	0.694 ± 0.003	± 0.022	
3.50 – 3.75	0.621 ± 0.003	± 0.020	
3.75 – 4.00	0.562 ± 0.003	± 0.018	
4.00 – 4.50	0.487 ± 0.002	± 0.016	
4.50 – 5.00	0.397 ± 0.002	± 0.013	
5.00 – 5.50	0.334 ± 0.002	± 0.011	
5.50 – 6.00	0.283 ± 0.002	± 0.010	
6.00 – 6.50	0.245 ± 0.001	± 0.008	
6.50 – 7.00	0.214 ± 0.001	± 0.007	
7.00 – 7.50	0.183 ± 0.001	± 0.006	
7.50 – 8.00	0.156 ± 0.001	± 0.005	
8.00 – 8.50	0.136 ± 0.001	± 0.004	
8.50 – 9.00	0.122 ± 0.001	± 0.004	
9.00 – 9.50	0.107 ± 0.001	± 0.003	
9.50 – 10.00	0.0975 ± 0.0009	± 0.0031	
10.00 – 11.00	0.0791 ± 0.0006	± 0.0025	
11.00 – 12.00	0.0644 ± 0.0005	± 0.0021	
12.00 – 13.00	0.0516 ± 0.0004	± 0.0017	
13.00 – 14.00	0.0407 ± 0.0004	± 0.0013	
14.00 – 15.00	0.0343 ± 0.0004	± 0.0011	
15.00 – 16.00	0.0283 ± 0.0003	± 0.0009	
16.00 – 17.00	0.0223 ± 0.0003	± 0.0007	
17.00 – 18.00	0.0197 ± 0.0003	± 0.0006	
18.00 – 19.00	0.0150 ± 0.0002	± 0.0005	
19.00 – 20.00	0.0123 ± 0.0002	± 0.0004	

Table 10: *Pions from uds events normalized to the total number of events N_E . The systematic uncertainties of different momentum bins in the overlap region are correlated.*

p interval [GeV/c]	$\frac{1}{N_E} \cdot \frac{dN}{dp}$	Δ_{stat}	Δ_{sys}
.30 - .35	$.170 \cdot 10^{+0} \pm$	$.110 \cdot 10^{-1} \pm$	$.594 \cdot 10^{-2}$
.35 - .40	$.214 \cdot 10^{+0} \pm$	$.890 \cdot 10^{-2} \pm$	$.749 \cdot 10^{-2}$
.40 - .45	$.250 \cdot 10^{+0} \pm$	$.679 \cdot 10^{-2} \pm$	$.874 \cdot 10^{-2}$
.45 - .50	$.259 \cdot 10^{+0} \pm$	$.738 \cdot 10^{-2} \pm$	$.905 \cdot 10^{-2}$
.50 - .55	$.249 \cdot 10^{+0} \pm$	$.178 \cdot 10^{-1} \pm$	$.871 \cdot 10^{-2}$
.60 - .65	$.321 \cdot 10^{+0} \pm$	$.706 \cdot 10^{-2} \pm$	$.112 \cdot 10^{-1}$
.65 - .70	$.321 \cdot 10^{+0} \pm$	$.709 \cdot 10^{-2} \pm$	$.112 \cdot 10^{-1}$
1.50 - 1.75	$.280 \cdot 10^{+0} \pm$	$.461 \cdot 10^{-2} \pm$	$.168 \cdot 10^{-1}$
1.75 - 2.00	$.256 \cdot 10^{+0} \pm$	$.486 \cdot 10^{-2} \pm$	$.154 \cdot 10^{-1}$
2.00 - 2.25	$.225 \cdot 10^{+0} \pm$	$.675 \cdot 10^{-2} \pm$	$.135 \cdot 10^{-1}$
3.75 - 4.00	$.938 \cdot 10^{-1} \pm$	$.270 \cdot 10^{-2} \pm$	$.563 \cdot 10^{-2}$
4.00 - 4.50	$.899 \cdot 10^{-1} \pm$	$.161 \cdot 10^{-2} \pm$	$.540 \cdot 10^{-2}$
4.50 - 5.00	$.782 \cdot 10^{-1} \pm$	$.147 \cdot 10^{-2} \pm$	$.469 \cdot 10^{-2}$
5.00 - 5.50	$.676 \cdot 10^{-1} \pm$	$.140 \cdot 10^{-2} \pm$	$.405 \cdot 10^{-2}$
5.50 - 6.00	$.592 \cdot 10^{-1} \pm$	$.126 \cdot 10^{-2} \pm$	$.355 \cdot 10^{-2}$
6.00 - 6.50	$.556 \cdot 10^{-1} \pm$	$.140 \cdot 10^{-2} \pm$	$.334 \cdot 10^{-2}$
6.50 - 7.00	$.499 \cdot 10^{-1} \pm$	$.110 \cdot 10^{-2} \pm$	$.300 \cdot 10^{-2}$
7.00 - 7.50	$.443 \cdot 10^{-1} \pm$	$.104 \cdot 10^{-2} \pm$	$.266 \cdot 10^{-2}$
7.50 - 8.00	$.417 \cdot 10^{-1} \pm$	$.101 \cdot 10^{-2} \pm$	$.250 \cdot 10^{-2}$
8.00 - 8.50	$.409 \cdot 10^{-1} \pm$	$.957 \cdot 10^{-3} \pm$	$.245 \cdot 10^{-2}$
8.50 - 9.00	$.336 \cdot 10^{-1} \pm$	$.950 \cdot 10^{-3} \pm$	$.202 \cdot 10^{-2}$
9.00 - 9.50	$.345 \cdot 10^{-1} \pm$	$.883 \cdot 10^{-3} \pm$	$.207 \cdot 10^{-2}$
9.50 - 10.00	$.290 \cdot 10^{-1} \pm$	$.806 \cdot 10^{-3} \pm$	$.174 \cdot 10^{-2}$
10.00 - 11.00	$.291 \cdot 10^{-1} \pm$	$.546 \cdot 10^{-3} \pm$	$.175 \cdot 10^{-2}$
11.00 - 12.00	$.228 \cdot 10^{-1} \pm$	$.479 \cdot 10^{-3} \pm$	$.137 \cdot 10^{-2}$
12.00 - 13.00	$.204 \cdot 10^{-1} \pm$	$.443 \cdot 10^{-3} \pm$	$.123 \cdot 10^{-2}$
13.00 - 14.00	$.177 \cdot 10^{-1} \pm$	$.414 \cdot 10^{-3} \pm$	$.106 \cdot 10^{-2}$
14.00 - 15.00	$.151 \cdot 10^{-1} \pm$	$.396 \cdot 10^{-3} \pm$	$.907 \cdot 10^{-3}$
15.00 - 16.00	$.130 \cdot 10^{-1} \pm$	$.352 \cdot 10^{-3} \pm$	$.777 \cdot 10^{-3}$
16.00 - 17.00	$.112 \cdot 10^{-1} \pm$	$.295 \cdot 10^{-3} \pm$	$.674 \cdot 10^{-3}$
17.00 - 18.00	$.946 \cdot 10^{-2} \pm$	$.291 \cdot 10^{-3} \pm$	$.568 \cdot 10^{-3}$
18.00 - 19.00	$.771 \cdot 10^{-2} \pm$	$.268 \cdot 10^{-3} \pm$	$.463 \cdot 10^{-3}$
19.00 - 20.00	$.704 \cdot 10^{-2} \pm$	$.240 \cdot 10^{-3} \pm$	$.422 \cdot 10^{-3}$

Table 11: *Kaons from uds events normalized to the total number of events N_E . The systematic uncertainties of different momentum bins in the overlap region are correlated.*

p interval [GeV/c]	$\frac{1}{N_E} \frac{dN}{dp}$	Δ_{stat}	Δ_{sys}
0.30 - 0.35	0.0319 ±	0.0058 ±	0.0010
0.35 - 0.40	0.0642 ±	0.0045 ±	0.0019
0.40 - 0.45	0.0806 ±	0.0046 ±	0.0024
0.45 - 0.50	0.102 ±	0.004 ±	0.003
0.50 - 0.55	0.110 ±	0.004 ±	0.003
0.55 - 0.60	0.131 ±	0.004 ±	0.004
0.60 - 0.65	0.127 ±	0.004 ±	0.004
0.65 - 0.70	0.148 ±	0.004 ±	0.004
0.80 - 0.90	0.149 ±	0.003 ±	0.004
0.90 - 1.00	0.150 ±	0.006 ±	0.004
1.00 - 1.10	0.159 ±	0.006 ±	0.005
1.10 - 1.20	0.158 ±	0.004 ±	0.005
3.50 - 3.75	0.0653 ±	0.0025 ±	0.0052
3.75 - 4.00	0.0595 ±	0.0019 ±	0.0048
4.00 - 4.50	0.0522 ±	0.0011 ±	0.0042
4.50 - 5.00	0.0461 ±	0.0010 ±	0.0037
5.00 - 5.50	0.0401 ±	0.0009 ±	0.0032
5.50 - 6.00	0.0345 ±	0.0008 ±	0.0028
6.00 - 6.50	0.0333 ±	0.0008 ±	0.0027
6.50 - 7.00	0.0297 ±	0.0007 ±	0.0024
7.00 - 7.50	0.0268 ±	0.0006 ±	0.0021
7.50 - 8.00	0.0245 ±	0.0006 ±	0.0020
8.00 - 8.50	0.0202 ±	0.0006 ±	0.0016
8.50 - 9.00	0.0190 ±	0.0005 ±	0.0015
9.00 - 9.50	0.0162 ±	0.0005 ±	0.0013
9.50 - 10.00	0.0166 ±	0.0005 ±	0.0013
10.00 - 11.00	0.0124 ±	0.0003 ±	0.0010
11.00 - 12.00	0.0115 ±	0.0003 ±	0.0009
12.00 - 13.00	0.00933 ±	0.00026 ±	0.00075
13.00 - 14.00	0.00746 ±	0.00026 ±	0.00060
14.00 - 15.00	0.00627 ±	0.00024 ±	0.00050
15.00 - 16.00	0.00561 ±	0.00021 ±	0.00045
16.00 - 17.00	0.00454 ±	0.00017 ±	0.00036
17.00 - 18.00	0.00404 ±	0.00016 ±	0.00032
18.00 - 19.00	0.00316 ±	0.00014 ±	0.00025
19.00 - 20.00	0.00287 ±	0.00013 ±	0.00023

Table 12: *Protons from uds events normalized to the total number of events N_E . The systematic uncertainties of different momentum bins in the overlap region are correlated.*

p interval [GeV/c]	$\frac{1}{N_E} \frac{dN}{dp}$	Δ_{stat}	Δ_{sys}
0.30 – 0.35	1.54 ± 0.05	± 0.120	
0.35 – 0.40	1.46 ± 0.05	± 0.12	
0.40 – 0.45	1.48 ± 0.04	± 0.12	
0.45 – 0.50	1.51 ± 0.04	± 0.12	
0.50 – 0.55	1.34 ± 0.04	± 0.11	
0.55 – 0.60	1.32 ± 0.03	± 0.11	
0.60 – 0.65	1.16 ± 0.03	± 0.09	
0.65 – 0.70	1.20 ± 0.03	± 0.10	
1.50 – 1.75	0.511 ± 0.021	± 0.041	
1.75 – 2.00	0.431 ± 0.017	± 0.035	
2.00 – 2.25	0.390 ± 0.010	± 0.031	
2.25 – 2.50	0.341 ± 0.008	± 0.027	
2.50 – 2.75	0.304 ± 0.007	± 0.024	
2.75 – 3.00	0.259 ± 0.008	± 0.021	
3.00 – 3.25	0.233 ± 0.005	± 0.019	
3.25 – 3.50	0.209 ± 0.005	± 0.017	
3.50 – 3.75	0.180 ± 0.005	± 0.014	
3.75 – 4.00	0.154 ± 0.004	± 0.012	
4.00 – 4.50	0.130 ± 0.003	± 0.010	
4.50 – 5.00	0.118 ± 0.003	± 0.009	
5.00 – 5.50	0.092 ± 0.002	± 0.007	
5.50 – 6.00	0.0816 ± 0.0021	± 0.0065	
6.00 – 6.50	0.0658 ± 0.0019	± 0.0053	
6.50 – 7.00	0.0555 ± 0.0018	± 0.0044	
7.00 – 7.50	0.0455 ± 0.0016	± 0.0036	
7.50 – 8.00	0.0430 ± 0.0015	± 0.0034	
8.00 – 8.50	0.0382 ± 0.0014	± 0.0031	
8.50 – 9.00	0.0300 ± 0.0013	± 0.0024	
9.00 – 9.50	0.0281 ± 0.0012	± 0.0023	
9.50 – 10.00	0.0209 ± 0.0011	± 0.0017	
10.00 – 11.00	0.0200 ± 0.0007	± 0.0016	
11.00 – 12.00	0.0143 ± 0.0006	± 0.0011	
12.00 – 13.00	0.0107 ± 0.0005	± 0.0009	
13.00 – 14.00	0.00941 ± 0.00048	± 0.00075	
14.00 – 15.00	0.00642 ± 0.00044	± 0.00051	
15.00 – 16.00	0.00419 ± 0.00045	± 0.00034	
16.00 – 17.00	0.00514 ± 0.00036	± 0.00041	
17.00 – 18.00	0.00289 ± 0.00034	± 0.00023	
18.00 – 19.00	0.00336 ± 0.00034	± 0.00027	
19.00 – 20.00	0.00242 ± 0.00029	± 0.00019	

Table 13: *Pions from c events normalized to the total number of events N_E . The systematic uncertainties of different momentum bins in the overlap region are correlated.*

p interval [GeV/c]	$\frac{1}{N_E} \frac{dN}{dp}$	Δ_{stat}	Δ_{sys}
0.30 - 0.35	0.0726 ±	0.0103 ±	0.0058
0.35 - 0.40	0.0588 ±	0.0085 ±	0.0047
0.40 - 0.45	0.0441 ±	0.0070 ±	0.0035
0.45 - 0.50	0.0603 ±	0.0084 ±	0.0048
0.50 - 0.55	0.0920 ±	0.0223 ±	0.0074
0.60 - 0.65	0.0636 ±	0.0081 ±	0.0051
0.65 - 0.70	0.0777 ±	0.0083 ±	0.0062
1.50 - 1.75	0.0790 ±	0.0057 ±	0.0095
1.75 - 2.00	0.0501 ±	0.0061 ±	0.0065
2.00 - 2.25	0.0674 ±	0.0085 ±	0.0108
3.75 - 4.00	0.0408 ±	0.0032 ±	0.0041
4.00 - 4.50	0.0309 ±	0.0020 ±	0.0031
4.50 - 5.00	0.0310 ±	0.0018 ±	0.0031
5.00 - 5.50	0.0309 ±	0.0016 ±	0.0031
5.50 - 6.00	0.0285 ±	0.0015 ±	0.0029
6.00 - 6.50	0.0212 ±	0.0015 ±	0.0021
6.50 - 7.00	0.0194 ±	0.0013 ±	0.0019
7.00 - 7.50	0.0201 ±	0.0012 ±	0.0020
7.50 - 8.00	0.0173 ±	0.0011 ±	0.0017
8.00 - 8.50	0.0146 ±	0.0011 ±	0.0015
8.50 - 9.00	0.0193 ±	0.0011 ±	0.0019
9.00 - 9.50	0.0121 ±	0.0009 ±	0.0012
9.50 - 10.00	0.0131 ±	0.0009 ±	0.0013
10.00 - 11.00	0.00808 ±	0.00057 ±	0.00081
11.00 - 12.00	0.00792 ±	0.00050 ±	0.00079
12.00 - 13.00	0.00736 ±	0.00044 ±	0.00074
13.00 - 14.00	0.00532 ±	0.00041 ±	0.00053
14.00 - 15.00	0.00554 ±	0.00039 ±	0.00055
15.00 - 16.00	0.00381 ±	0.00036 ±	0.00038
16.00 - 17.00	0.00252 ±	0.00029 ±	0.00025
17.00 - 18.00	0.00330 ±	0.00028 ±	0.00033
18.00 - 19.00	0.00251 ±	0.00027 ±	0.00025
19.00 - 20.00	0.00165 ±	0.00023 ±	0.00017

Table 14: *Kaons from c events normalized to the total number of events N_E . The systematic uncertainties of different momentum bins in the overlap region are correlated.*

p interval [GeV/c]	$\frac{1}{N_E} \frac{dN}{dp}$	Δ_{stat}	Δ_{sys}
0.30 – 0.35	0.00073 ±	0.00530 ±	0.00062
0.35 – 0.40	0.0092 ±	0.0043 ±	0.0007
0.40 – 0.45	0.0350 ±	0.0047 ±	0.0028
0.45 – 0.50	0.0247 ±	0.0044 ±	0.0020
0.50 – 0.55	0.0287 ±	0.0047 ±	0.0023
0.55 – 0.60	0.0308 ±	0.0047 ±	0.0025
0.60 – 0.65	0.0334 ±	0.0048 ±	0.0027
0.65 – 0.70	0.0321 ±	0.0052 ±	0.0026
0.80 – 0.90	0.0395 ±	0.0040 ±	0.0032
0.90 – 1.00	0.0513 ±	0.0078 ±	0.0041
1.00 – 1.10	0.0413 ±	0.0069 ±	0.0033
1.10 – 1.20	0.0414 ±	0.0048 ±	0.0033
3.50 – 3.75	0.0133 ±	0.0032 ±	0.0015
3.75 – 4.00	0.0165 ±	0.0023 ±	0.0018
4.00 – 4.50	0.0146 ±	0.0014 ±	0.0016
4.50 – 5.00	0.0101 ±	0.0012 ±	0.0011
5.00 – 5.50	0.00850 ±	0.00107 ±	0.00094
5.50 – 6.00	0.00896 ±	0.00095 ±	0.00099
6.00 – 6.50	0.00783 ±	0.00091 ±	0.00086
6.50 – 7.00	0.00593 ±	0.00082 ±	0.00065
7.00 – 7.50	0.00303 ±	0.00076 ±	0.00033
7.50 – 8.00	0.00297 ±	0.00071 ±	0.00033
8.00 – 8.50	0.00530 ±	0.00066 ±	0.00058
8.50 – 9.00	0.00254 ±	0.00065 ±	0.00028
9.00 – 9.50	0.00287 ±	0.00058 ±	0.00032
9.50 – 10.00	0.00134 ±	0.00056 ±	0.00015
10.00 – 11.00	0.00315 ±	0.00035 ±	0.00035
11.00 – 12.00	0.00127 ±	0.00032 ±	0.00014
12.00 – 13.00	0.00130 ±	0.00026 ±	0.00014
13.00 – 14.00	0.00152 ±	0.00025 ±	0.00017
14.00 – 15.00	0.000853 ±	0.000227 ±	0.000094
15.00 – 16.00	0.000116 ±	0.000208 ±	0.000013
16.00 – 17.00	0.000290 ±	0.000159 ±	0.000032
17.00 – 18.00	-.000016 ±	0.000148 ±	0.000002
18.00 – 19.00	0.000103 ±	0.000131 ±	0.000011
19.00 – 20.00	-.000170 ±	0.000120 ±	0.000019

Table 15: *Protons from c events normalized to the total number of events N_E . The systematic uncertainties of different momentum bins in the overlap region are correlated.*

p interval [GeV/c]	$\frac{1}{N_E} \frac{dN}{dp}$	Δ_{stat}	Δ_{sys}
0.30 - 0.35	2.41 ± 0.02	± 0.07	
0.35 - 0.40	2.46 ± 0.02	± 0.08	
0.40 - 0.45	2.42 ± 0.02	± 0.08	
0.45 - 0.50	2.29 ± 0.01	± 0.07	
0.50 - 0.55	2.22 ± 0.01	± 0.07	
0.55 - 0.60	2.09 ± 0.01	± 0.06	
0.60 - 0.65	2.03 ± 0.01	± 0.06	
0.65 - 0.70	1.87 ± 0.01	± 0.06	
1.50 - 1.75	0.817 ± 0.008	± 0.029	
1.75 - 2.00	0.657 ± 0.007	± 0.024	
2.00 - 2.25	0.573 ± 0.004	± 0.021	
2.25 - 2.50	0.492 ± 0.003	± 0.018	
2.50 - 2.75	0.415 ± 0.003	± 0.015	
2.75 - 3.00	0.372 ± 0.003	± 0.013	
3.00 - 3.25	0.317 ± 0.002	± 0.011	
3.25 - 3.50	0.277 ± 0.002	± 0.010	
3.50 - 3.75	0.248 ± 0.002	± 0.009	
3.75 - 4.00	0.220 ± 0.002	± 0.008	
4.00 - 4.50	0.186 ± 0.001	± 0.007	
4.50 - 5.00	0.144 ± 0.001	± 0.005	
5.00 - 5.50	0.118 ± 0.001	± 0.004	
5.50 - 6.00	0.0950 ± 0.0008	± 0.0034	
6.00 - 6.50	0.0757 ± 0.0007	± 0.0027	
6.50 - 7.00	0.0632 ± 0.0006	± 0.0023	
7.00 - 7.50	0.0530 ± 0.0006	± 0.0019	
7.50 - 8.00	0.0421 ± 0.0005	± 0.0015	
8.00 - 8.50	0.0349 ± 0.0005	± 0.0013	
8.50 - 9.00	0.0296 ± 0.0004	± 0.0011	
9.00 - 9.50	0.0256 ± 0.0004	± 0.0009	
9.50 - 10.00	0.0225 ± 0.0004	± 0.0008	
10.00 - 11.00	0.0164 ± 0.0002	± 0.0006	
11.00 - 12.00	0.0131 ± 0.0002	± 0.0005	
12.00 - 13.00	0.0100 ± 0.0002	± 0.0004	
13.00 - 14.00	0.00691 ± 0.00015	± 0.00025	
14.00 - 15.00	0.00547 ± 0.00014	± 0.00020	
15.00 - 16.00	0.00505 ± 0.00018	± 0.00018	
16.00 - 17.00	0.00321 ± 0.00012	± 0.00012	
17.00 - 18.00	0.00255 ± 0.00013	± 0.00009	
18.00 - 19.00	0.00205 ± 0.00011	± 0.00007	
19.00 - 20.00	0.00150 ± 0.00011	± 0.00005	

Table 16: *Pions from b events normalized to the total number of events N_E . The systematic uncertainties of different momentum bins in the overlap region are correlated.*

p interval [GeV/c]	$\frac{1}{N_E} \frac{dN}{dp}$	Δ_{stat}	Δ_{sys}
0.30 – 0.35	0.0601 ±	0.0035 ±	0.0024
0.35 – 0.40	0.0772 ±	0.0032 ±	0.0031
0.40 – 0.45	0.0837 ±	0.0027 ±	0.0034
0.45 – 0.50	0.0855 ±	0.0032 ±	0.0034
0.50 – 0.55	0.108 ±	0.008 ±	0.004
0.60 – 0.65	0.116 ±	0.003 ±	0.005
0.65 – 0.70	0.120 ±	0.003 ±	0.005
1.50 – 1.75	0.133 ±	0.002 ±	0.009
1.75 – 2.00	0.123 ±	0.002 ±	0.011
2.00 – 2.25	0.115 ±	0.003 ±	0.016
3.75 – 4.00	0.0536 ±	0.0012 ±	0.0032
4.00 – 4.50	0.0513 ±	0.0008 ±	0.0031
4.50 – 5.00	0.0438 ±	0.0007 ±	0.0026
5.00 – 5.50	0.0360 ±	0.0006 ±	0.0022
5.50 – 6.00	0.0327 ±	0.0006 ±	0.0020
6.00 – 6.50	0.0296 ±	0.0005 ±	0.0018
6.50 – 7.00	0.0250 ±	0.0005 ±	0.0015
7.00 – 7.50	0.0206 ±	0.0004 ±	0.0012
7.50 – 8.00	0.0183 ±	0.0004 ±	0.0011
8.00 – 8.50	0.0162 ±	0.0004 ±	0.0010
8.50 – 9.00	0.0134 ±	0.0004 ±	0.0008
9.00 – 9.50	0.0121 ±	0.0003 ±	0.0007
9.50 – 10.00	0.00923 ±	0.00030 ±	0.00055
10.00 – 11.00	0.00883 ±	0.00020 ±	0.00053
11.00 – 12.00	0.00581 ±	0.00017 ±	0.00035
12.00 – 13.00	0.00440 ±	0.00014 ±	0.00026
13.00 – 14.00	0.00366 ±	0.00013 ±	0.00022
14.00 – 15.00	0.00242 ±	0.00012 ±	0.00015
15.00 – 16.00	0.00186 ±	0.00012 ±	0.00011
16.00 – 17.00	0.00153 ±	0.00009 ±	0.00009
17.00 – 18.00	0.00107 ±	0.00009 ±	0.00006
18.00 – 19.00	0.000671 ±	0.000074 ±	0.000040
19.00 – 20.00	0.000639 ±	0.000065 ±	0.000038

Table 17: *Kaons from b events normalized to the total number of events N_E . The systematic uncertainties of different momentum bins in the overlap region are correlated.*

p interval [GeV/c]	$\frac{1}{N_E} \frac{dN}{dp}$	Δ_{stat}	Δ_{sys}
0.30 – 0.35	0.0123 ±	0.0024 ±	0.0005
0.35 – 0.40	0.0241 ±	0.0017 ±	0.0010
0.40 – 0.45	0.0284 ±	0.0016 ±	0.0011
0.45 – 0.50	0.0353 ±	0.0017 ±	0.0014
0.50 – 0.55	0.0413 ±	0.0018 ±	0.0017
0.55 – 0.60	0.0400 ±	0.0017 ±	0.0016
0.60 – 0.65	0.0438 ±	0.0018 ±	0.0018
0.65 – 0.70	0.0525 ±	0.0020 ±	0.0021
0.80 – 0.90	0.0511 ±	0.0015 ±	0.0020
0.90 – 1.00	0.0616 ±	0.0030 ±	0.0025
1.00 – 1.10	0.0565 ±	0.0029 ±	0.0023
1.10 – 1.20	0.0631 ±	0.0018 ±	0.0025
3.50 – 3.75	0.0290 ±	0.0013 ±	0.0026
3.75 – 4.00	0.0237 ±	0.0009 ±	0.0021
4.00 – 4.50	0.0189 ±	0.0005 ±	0.0017
4.50 – 5.00	0.0175 ±	0.0005 ±	0.0016
5.00 – 5.50	0.0152 ±	0.0004 ±	0.0014
5.50 – 6.00	0.0116 ±	0.0004 ±	0.0010
6.00 – 6.50	0.0102 ±	0.0003 ±	0.0010
6.50 – 7.00	0.00988 ±	0.00031 ±	0.00089
7.00 – 7.50	0.00903 ±	0.00029 ±	0.00081
7.50 – 8.00	0.00787 ±	0.00027 ±	0.00071
8.00 – 8.50	0.00591 ±	0.00024 ±	0.00053
8.50 – 9.00	0.00618 ±	0.00024 ±	0.00056
9.00 – 9.50	0.00476 ±	0.00022 ±	0.00043
9.50 – 10.00	0.00469 ±	0.00021 ±	0.00042
10.00 – 11.00	0.00313 ±	0.00013 ±	0.00028
11.00 – 12.00	0.00277 ±	0.00012 ±	0.00025
12.00 – 13.00	0.00154 ±	0.00009 ±	0.00014
13.00 – 14.00	0.00113 ±	0.00007 ±	0.00010
14.00 – 15.00	0.00102 ±	0.00007 ±	0.00009
15.00 – 16.00	0.000915 ±	0.000073 ±	0.000082
16.00 – 17.00	0.000490 ±	0.000055 ±	0.000044
17.00 – 18.00	0.000406 ±	0.000053 ±	0.000037
18.00 – 19.00	0.000245 ±	0.000041 ±	0.000022
19.00 – 20.00	0.000305 ±	0.000041 ±	0.000028

Table 18: *Protons from b events normalized to the total number of events N_E . The systematic uncertainties of different momentum bins in the overlap region are correlated.*

p interval [GeV/c]	$\frac{1}{N_E} \frac{dN}{dp}$	Δ_{stat}	Δ_{sys}
0.30 – 0.35	0.330 ±	0.017 ±	0.017
0.35 – 0.40	0.482 ±	0.014 ±	0.024
0.40 – 0.45	0.548 ±	0.013 ±	0.027
0.45 – 0.50	0.605 ±	0.013 ±	0.030
0.50 – 0.55	0.580 ±	0.012 ±	0.029
0.55 – 0.60	0.601 ±	0.012 ±	0.030
0.60 – 0.65	0.651 ±	0.012 ±	0.033
0.65 – 0.70	0.604 ±	0.012 ±	0.030
1.50 – 1.75	0.393 ±	0.009 ±	0.020
1.75 – 2.00	0.307 ±	0.009 ±	0.015
2.00 – 2.25	0.302 ±	0.006 ±	0.015
2.25 – 2.50	0.285 ±	0.005 ±	0.014
2.50 – 2.75	0.253 ±	0.005 ±	0.013
2.75 – 3.00	0.227 ±	0.004 ±	0.011
3.00 – 3.25	0.202 ±	0.003 ±	0.010
3.25 – 3.50	0.183 ±	0.003 ±	0.009
3.50 – 3.75	0.163 ±	0.003 ±	0.008
3.75 – 4.00	0.149 ±	0.003 ±	0.007
4.00 – 4.50	0.129 ±	0.002 ±	0.006
4.50 – 5.00	0.101 ±	0.002 ±	0.005
5.00 – 5.50	0.0848 ±	0.0016 ±	0.0042
5.50 – 6.00	0.0722 ±	0.0015 ±	0.0036
6.00 – 6.50	0.0583 ±	0.0013 ±	0.0029
6.50 – 7.00	0.0502 ±	0.0012 ±	0.0025
7.00 – 7.50	0.0425 ±	0.0012 ±	0.0021
7.50 – 8.00	0.0336 ±	0.0010 ±	0.0017
8.00 – 8.50	0.0281 ±	0.0010 ±	0.0014
8.50 – 9.00	0.0245 ±	0.0009 ±	0.0012
9.00 – 9.50	0.0212 ±	0.0009 ±	0.0011
9.50 – 10.00	0.0186 ±	0.0008 ±	0.0009
10.00 – 11.00	0.0141 ±	0.0005 ±	0.0007
11.00 – 12.00	0.0112 ±	0.0004 ±	0.0006
12.00 – 13.00	0.00893 ±	0.00039 ±	0.00045
13.00 – 14.00	0.00573 ±	0.00033 ±	0.00029
14.00 – 15.00	0.00466 ±	0.00030 ±	0.00023
15.00 – 16.00	0.00478 ±	0.00033 ±	0.00024
16.00 – 17.00	0.00286 ±	0.00024 ±	0.00014
17.00 – 18.00	0.00219 ±	0.00024 ±	0.00011
18.00 – 19.00	0.00200 ±	0.00025 ±	0.00010
19.00 – 20.00	0.000739 ±	0.000166 ±	0.000037

Table 19: *Pions from b-hadron decays normalized to the total number of events N_E . The systematic uncertainties of different momentum bins in the overlap region are correlated.*

p interval [GeV/c]	$\frac{1}{N_E} \frac{dN}{dp}$	Δ_{stat}	Δ_{sys}
0.30 – 0.35	−.0174 ±	0.0092 ±	0.0009
0.35 – 0.40	−.00368 ±	0.0085 ±	0.00065
0.40 – 0.45	0.00331 ±	0.00735 ±	0.00087
0.45 – 0.50	0.0191 ±	0.0091 ±	0.001
0.50 – 0.55	0.00656 ±	0.02480 ±	0.00033
0.60 – 0.65	0.0284 ±	0.0078 ±	0.0014
0.65 – 0.70	0.0101 ±	0.0076 ±	0.0005
1.50 – 1.75	0.0536 ±	0.0044 ±	0.0054
1.75 – 2.00	0.0466 ±	0.0045 ±	0.0051
2.00 – 2.25	0.0596 ±	0.0061 ±	0.0089
3.75 – 4.00	0.0436 ±	0.0023 ±	0.0035
4.00 – 4.50	0.0387 ±	0.0014 ±	0.0031
4.50 – 5.00	0.0330 ±	0.0013 ±	0.0026
5.00 – 5.50	0.0288 ±	0.0012 ±	0.0023
5.50 – 6.00	0.0263 ±	0.0011 ±	0.0021
6.00 – 6.50	0.0250 ±	0.0010 ±	0.0020
6.50 – 7.00	0.0196 ±	0.0009 ±	0.0016
7.00 – 7.50	0.0172 ±	0.0009 ±	0.0014
7.50 – 8.00	0.0154 ±	0.0008 ±	0.0012
8.00 – 8.50	0.0137 ±	0.0008 ±	0.0011
8.50 – 9.00	0.0118 ±	0.0007 ±	0.0009
9.00 – 9.50	0.0103 ±	0.0007 ±	0.0008
9.50 – 10.00	0.00774 ±	0.00062 ±	0.00062
10.00 – 11.00	0.00773 ±	0.00041 ±	0.00062
11.00 – 12.00	0.00457 ±	0.00036 ±	0.00037
12.00 – 13.00	0.00326 ±	0.00031 ±	0.00026
13.00 – 14.00	0.00263 ±	0.00028 ±	0.00021
14.00 – 15.00	0.00216 ±	0.00027 ±	0.00017
15.00 – 16.00	0.00157 ±	0.00027 ±	0.00013
16.00 – 17.00	0.00113 ±	0.00021 ±	0.00009
17.00 – 18.00	0.000801 ±	0.000201 ±	0.000064
18.00 – 19.00	0.000584 ±	0.000188 ±	0.000047
19.00 – 20.00	0.000601 ±	0.000157 ±	0.000048

Table 20: *Kaons from b-hadron decays normalized to the total number of events N_E . The systematic uncertainties of different momentum bins in the overlap region are correlated.*

p interval [GeV/c]	$\frac{1}{N_E} \frac{dN}{dp}$	Δ_{stat}	Δ_{sys}
3.75 – 4.00	0.00754 ±	0.00212 ±	0.00060
4.00 – 4.50	0.00741 ±	0.00126 ±	0.00059
4.50 – 5.00	0.00874 ±	0.00107 ±	0.00070
5.00 – 5.50	0.00832 ±	0.00095 ±	0.00067
5.50 – 6.00	0.00818 ±	0.00084 ±	0.00066
6.00 – 6.50	0.00506 ±	0.00076 ±	0.00041
6.50 – 7.00	0.00727 ±	0.00072 ±	0.00058
7.00 – 7.50	0.00615 ±	0.00067 ±	0.00049
7.50 – 8.00	0.00531 ±	0.00063 ±	0.00043
8.00 – 8.50	0.00394 ±	0.00057 ±	0.00032
8.50 – 9.00	0.00384 ±	0.00058 ±	0.00031
9.00 – 9.50	0.00285 ±	0.00052 ±	0.00023
9.50 – 10.00	0.00347 ±	0.00052 ±	0.00028
10.00 – 11.00	0.00203 ±	0.00031 ±	0.00016
11.00 – 12.00	0.00189 ±	0.00029 ±	0.00015
12.00 – 13.00	0.00137 ±	0.00023 ±	0.00011
13.00 – 14.00	0.000938 ±	0.00020 ±	0.00008
14.00 – 15.00	0.00106 ±	0.00020 ±	0.00009
15.00 – 16.00	0.000868 ±	0.000196 ±	0.000069
16.00 – 17.00	0.000528 ±	0.000145 ±	0.000042
17.00 – 18.00	0.000434 ±	0.000137 ±	0.000035
18.00 – 19.00	0.000068 ±	0.000112 ±	0.000005
19.00 – 20.00	0.000113 ±	0.000081 ±	0.000009

Table 21: *Protons from b-hadron decays normalized to the total number of events N_E . The systematic uncertainties of different momentum bins in the overlap region are correlated.*

p interval [GeV/c]	$\frac{1}{N_E} \frac{dN}{dp}$	Δ_{stat}	Δ_{sys}
0.30 – 0.35	2.12 ±	0.03 ±	0.11
0.35 – 0.40	1.97 ±	0.02 ±	0.10
0.40 – 0.45	1.86 ±	0.02 ±	0.10
0.45 – 0.50	1.67 ±	0.02 ±	0.08
0.50 – 0.55	1.63 ±	0.02 ±	0.08
0.55 – 0.60	1.47 ±	0.02 ±	0.07
0.60 – 0.65	1.35 ±	0.02 ±	0.07
0.65 – 0.70	1.24 ±	0.02 ±	0.06
1.50 – 1.75	0.405 ±	0.014 ±	0.020
1.75 – 2.00	0.346 ±	0.012 ±	0.017
2.00 – 2.25	0.263 ±	0.008 ±	0.013
2.25 – 2.50	0.201 ±	0.006 ±	0.010
2.50 – 2.75	0.157 ±	0.006 ±	0.008
2.75 – 3.00	0.137 ±	0.005 ±	0.007
3.00 – 3.25	0.112 ±	0.004 ±	0.006
3.25 – 3.50	0.0913 ±	0.0041 ±	0.0046
3.50 – 3.75	0.0841 ±	0.0039 ±	0.0042
3.75 – 4.00	0.0701 ±	0.0036 ±	0.0035
4.00 – 4.50	0.0550 ±	0.0024 ±	0.0028
4.50 – 5.00	0.0420 ±	0.0022 ±	0.0021
5.00 – 5.50	0.0330 ±	0.0020 ±	0.0017
5.50 – 6.00	0.0223 ±	0.0018 ±	0.0011
6.00 – 6.50	0.0169 ±	0.0017 ±	0.0008
6.50 – 7.00	0.0127 ±	0.0015 ±	0.0006
7.00 – 7.50	0.0102 ±	0.0014 ±	0.0005
7.50 – 8.00	0.00796 ±	0.00128 ±	0.00040
8.00 – 8.50	0.00613 ±	0.00117 ±	0.00031
8.50 – 9.00	0.00493 ±	0.00109 ±	0.00025
9.00 – 9.50	0.00434 ±	0.00103 ±	0.00022
9.50 – 10.00	0.00387 ±	0.00096 ±	0.00019
10.00 – 11.00	0.00222 ±	0.00059 ±	0.00011
11.00 – 12.00	0.00192 ±	0.00053 ±	0.00010
12.00 – 13.00	0.00121 ±	0.00045 ±	0.00006
13.00 – 14.00	0.00122 ±	0.00038 ±	0.00006
14.00 – 15.00	0.000793 ±	0.000342 ±	0.000040
15.00 – 16.00	0.000194 ±	0.000372 ±	0.000010
16.00 – 17.00	0.000349 ±	0.000275 ±	0.000017
17.00 – 18.00	0.000381 ±	0.000271 ±	0.000019
18.00 – 19.00	0.000106 ±	0.000272 ±	0.000005
19.00 – 20.00	0.000636 ±	0.000191 ±	0.000032

Table 22: *Accompanying pions in b events normalized to the total number of events N_E . The systematic uncertainties of different momentum bins in the overlap region are correlated.*

p interval [GeV/c]	$\frac{1}{N_E} \frac{dN}{dp}$	Δ_{stat}	Δ_{sys}
0.30 – 0.35	0.0789 ±	0.0113 ±	0.0040
0.35 – 0.40	0.0823 ±	0.0103 ±	0.0041
0.40 – 0.45	0.0819 ±	0.0087 ±	0.0041
0.45 – 0.50	0.0643 ±	0.0107 ±	0.0032
0.50 – 0.55	0.101 ±	0.029 ±	0.005
0.60 – 0.65	0.0881 ±	0.0094 ±	0.0044
0.65 – 0.70	0.110 ±	0.009 ±	0.006
1.50 – 1.75	0.0784 ±	0.0055 ±	0.0086
1.75 – 2.00	0.0768 ±	0.0057 ±	0.0100
2.00 – 2.25	0.0555 ±	0.0077 ±	0.0089
3.75 – 4.00	0.00934 ±	0.00291 ±	0.00075
4.00 – 4.50	0.0122 ±	0.0018 ±	0.0010
4.50 – 5.00	0.0106 ±	0.0016 ±	0.0008
5.00 – 5.50	0.00690 ±	0.00144 ±	0.00055
5.50 – 6.00	0.00615 ±	0.00134 ±	0.00049
6.00 – 6.50	0.00429 ±	0.00124 ±	0.00034
6.50 – 7.00	0.00563 ±	0.00114 ±	0.00045
7.00 – 7.50	0.00315 ±	0.00106 ±	0.00025
7.50 – 8.00	0.00311 ±	0.00099 ±	0.00025
8.00 – 8.50	0.00273 ±	0.00093 ±	0.00022
8.50 – 9.00	0.00158 ±	0.00090 ±	0.00013
9.00 – 9.50	0.00176 ±	0.00083 ±	0.00014
9.50 – 10.00	0.00154 ±	0.00074 ±	0.00012
10.00 – 11.00	0.00104 ±	0.00050 ±	0.00008
11.00 – 12.00	0.00122 ±	0.00043 ±	0.00010
12.00 – 13.00	0.00119 ±	0.00037 ±	0.00010
13.00 – 14.00	0.00105 ±	0.00034 ±	0.00008
14.00 – 15.00	0.000256 ±	0.000314 ±	0.000020
15.00 – 16.00	0.000384 ±	0.000314 ±	0.000031
16.00 – 17.00	0.000438 ±	0.000245 ±	0.000035
17.00 – 18.00	0.000239 ±	0.000239 ±	0.000019
18.00 – 19.00	0.000103 ±	0.000218 ±	0.000008
19.00 – 20.00	0.000015 ±	0.000187 ±	0.000001

Table 23: *Accompanying kaons in b events normalized to the total number of events N_E . The systematic uncertainties of different momentum bins in the overlap region are correlated.*

p interval [GeV/c]	$\frac{1}{N_E} \frac{dN}{dp}$	Δ_{stat}	Δ_{sys}
0.30 – 0.35	0.00190 ±	0.00050 ±	0.00010
0.35 – 0.40	0.0218 ±	0.0011 ±	0.0011
0.40 – 0.45	0.0200 ±	0.0010 ±	0.0010
0.45 – 0.50	0.0357 ±	0.0013 ±	0.0018
0.50 – 0.55	0.0421 ±	0.0014 ±	0.0021
0.55 – 0.60	0.0396 ±	0.0013 ±	0.0020
0.60 – 0.65	0.0371 ±	0.0012 ±	0.0019
0.65 – 0.70	0.0444 ±	0.0014 ±	0.0022
0.80 – 0.90	0.0509 ±	0.0012 ±	0.0025
0.90 – 1.00	0.0645 ±	0.0025 ±	0.0032
1.00 – 1.10	0.0574 ±	0.0022 ±	0.0029
1.10 – 1.20	0.0621 ±	0.0014 ±	0.0031
3.50 – 3.75	0.0206 ±	0.0007 ±	0.0016
3.75 – 4.00	0.0162 ±	0.0026 ±	0.0013
4.00 – 4.50	0.0112 ±	0.0015 ±	0.0009
4.50 – 5.00	0.00849 ±	0.00131 ±	0.00068
5.00 – 5.50	0.00690 ±	0.00116 ±	0.00055
5.50 – 6.00	0.00316 ±	0.00103 ±	0.00025
6.00 – 6.50	0.00495 ±	0.00093 ±	0.00040
6.50 – 7.00	0.00241 ±	0.00089 ±	0.00019
7.00 – 7.50	0.00303 ±	0.00082 ±	0.00024
7.50 – 8.00	0.00244 ±	0.00077 ±	0.00020
8.00 – 8.50	0.00198 ±	0.00070 ±	0.00016
8.50 – 9.00	0.00236 ±	0.00070 ±	0.00019
9.00 – 9.50	0.00200 ±	0.00062 ±	0.00016
9.50 – 10.00	0.00111 ±	0.00062 ±	0.00009
10.00 – 11.00	0.00108 ±	0.00037 ±	0.00009
11.00 – 12.00	0.000855 ±	0.000344 ±	0.000068
12.00 – 13.00	0.000130 ±	0.000264 ±	0.000010
13.00 – 14.00	0.000225 ±	0.000233 ±	0.000018
14.00 – 15.00	0.000042 ±	0.000231 ±	0.000003
15.00 – 16.00	0.000031 ±	0.000222 ±	0.000003
16.00 – 17.00	0.000041 ±	0.000165 ±	0.000003
17.00 – 18.00	0.000035 ±	0.000153 ±	0.000003
18.00 – 19.00	0.000203 ±	0.000123 ±	0.000016
19.00 – 20.00	0.000444 ±	0.000092 ±	0.000035

Table 24: *Accompanying protons in b events normalized to the total number of events N_E . The systematic uncertainties of different momentum bins in the overlap region are correlated.*

References

- [1] I. I. Bigi, B. Blok, M. Shifman, A. Vainshtein, CERN – TH 7082/93.
- [2] E. Bagan, P. Ball, V. M. Braun, P. Gosdzinsky, Nucl. Phys. **B 432** (1994) 3; Phys. Lett. **B 342**, (1995) 362;
E. Bagan, P. Ball, B. Fiol, P. Gosdzinsky, Phys. Lett. **B 351** (1995) 546.
- [3] for a review see e.g. M. Neubert, CERN – TH/96 – 55 (1996), to appear in International Journal of Modern Physics A, and references there.
- [4] Particle Data Group, “*Review of Particle Physics*”, Phys.Rev. **D 54** (1996) 1.
- [5] ALEPH collaboration,
“*ALEPH: A Detector for Electron-Positron Annihilations at LEP*”, NIM **A 294** (1990) 121.
- [6] ALEPH collaboration, “*Performance of the ALEPH detector at LEP*”, NIM **A 360** (1995) 481.
- [7] ALEPH collaboration, “*Inclusive π^\pm , K^\pm , (p, \bar{p}) differential cross-sections at the Z resonance*”, Z. Phys. **C 66** (1995) 355.
- [8] ALEPH collaboration, “*Update of Electroweak Parameters from Z Decays*”, Z. Phys. **C 60** (1993) 71.
- [9] W. B. Atwood et al., NIM **A 306** (1991) 446.
- [10] H. A. Bethe, Ann. Phys. **5** (1930) 324;
F. Bloch, Z. Phys. **81** (1933) 363.
- [11] ALEPH collaboration, “*A precise measurement of $\Gamma_{Z \rightarrow b\bar{b}/Z \rightarrow \text{hadrons}}$* ”, Phys. Lett. **B 313** (1993) 535.
- [12] J. E. Campagne and R. Zitoun, Z. Phys. **C 42** (1989) 469.
- [13] T. Sjöstrand, Computer Physics Commun. **39** (1986) 347;
M. Bengtsson and T. Sjöstrand, Computer Physics Commun. **43** (1987) 367.
- [14] ALEPH collaboration, “*Properties of Hadronic Z Decays and Test of QCD Generators*”, Z. Phys. **C 55** (1992) 209.
- [15] http://alephwww.cern.ch/ALPUB/paper/paper_97.html
- [16] DELPHI collaboration, “*Inclusive Measurements of the K^\pm and p, \bar{p} Production in Hadronic Z^0 Decays*”, Nucl. Phys. **B 444** (1995) 3.
- [17] OPAL collaboration, “*Measurement of the Production Rates of Charged Hadrons in e^+e^- Annihilation at the Z^0* ”, Z. Phys. **C 63** (1994) 181.

- [18] DELPHI collaboration, “*Production of Charged Particles, K_S^0 , K^\pm , p and Λ in $Z \rightarrow b\bar{b}$ Events and in the Decay of b Hadrons*”, Phys. Lett. **B 347** (1995) 447.
- [19] ALEPH collaboration, “*Heavy flavour production and decay with prompt leptons in the ALEPH detector*”, Z. Phys. **C 62** (1994) 179.
- [20] ALEPH collaboration, “*Measurement of the b forward-backward asymmetry and mixing using high- p_\perp leptons*”, Phys. Lett. **B 384** (1996) 414.
- [21] OPAL collaboration, “*Studies of Charged Particle Multiplicities in b Quark Events*”, Z. Phys. **C 61** (1994) 209.
- [22] ALEPH collaboration, “*Heavy quark tagging with leptons in the ALEPH detector*”, NIM **A 346** (1994) 461.
- [23] DELPHI collaboration, “*Lifetime and production rate of beauty baryons from Z decays*”, Z. Phys. **C 68** (1995) 375.
- [24] OPAL collaboration, “*Measurement of the Semileptonic Branching Fraction of Inclusive b Baryon Decays to Λ* ”, Z. Phys. **C 74** (1997) 423.
- [25] ARGUS collaboration, “*Inclusive production of charged pions, kaons and protons in $\Upsilon(4S)$ decays*”, Z. Phys. **C 58** (1993) 191.
- [26] CLEO collaboration, “*Measurement of baryon production in B meson decay*”, Phys. Rev. **D 45** (1992) 752.
- [27] ALEPH collaboration, “*Measurement of the Λ_b polarization in Z decays*”, Phys. Lett. **B 365** (1996) 437.